Accepted Manuscript

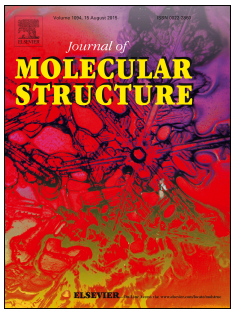

Spectroscopic and theoretical studies of some 2-(2′-haloacetyl)-5-substituted: 1-Methylpyrrole, furan and thiophene

Jéssica Valença, Daniel N.S. Rodrigues, Paulo R. Olivato, Maurizio Dal Colle

PII: S0022-2860(17)31242-5

DOI: 10.1016/j.molstruc.2017.09.055

Reference: MOLSTR 24304

To appear in: *Journal of Molecular Structure*

Received Date: 2 August 2017

Revised Date: 16 September 2017

Accepted Date: 18 September 2017

Please cite this article as: Jé. Valença, D.N.S. Rodrigues, P.R. Olivato, M. Dal Colle, Spectroscopic and theoretical studies of some 2-(2′-haloacetyl)-5-substituted: 1-Methylpyrrole, furan and thiophene, *Journal of Molecular Structure* (2017), doi: 10.1016/j.molstruc.2017.09.055.

Most stable conformers in the gas phase for compounds **1-7.**

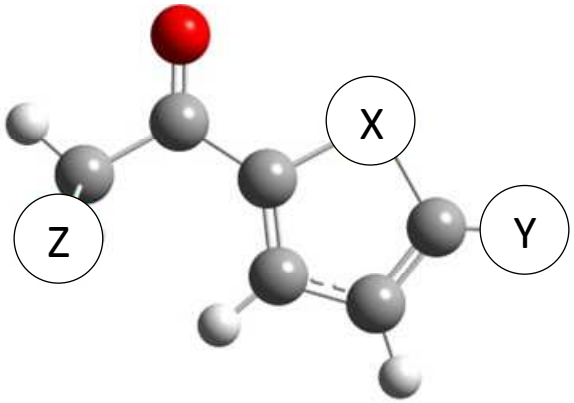

ac(*syn*)

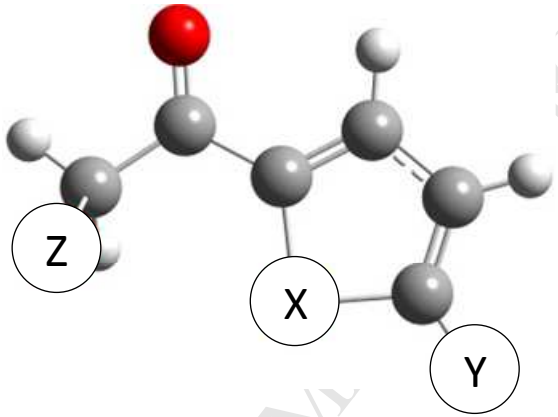

ac(*anti*)

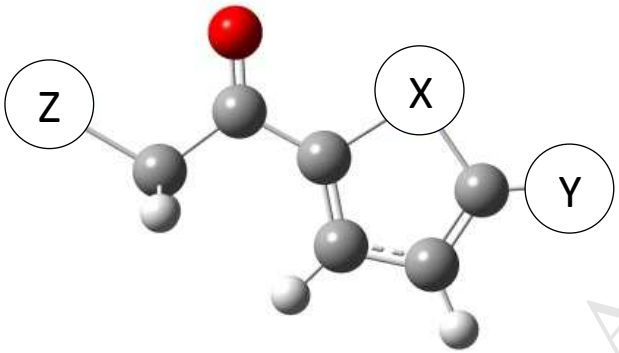

sp(*syn*)

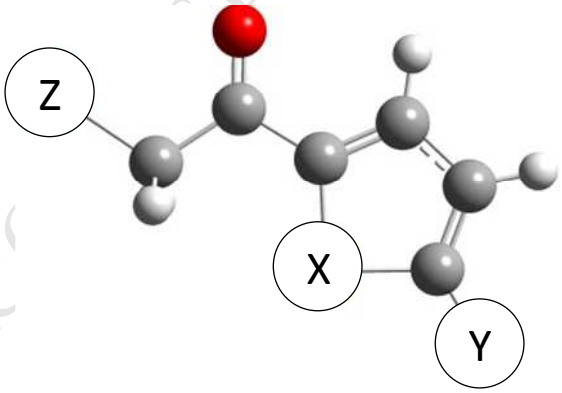

sp(*anti*)

= H

= C

= O

X = (NMe, O, S)

Y = (H, Me, Cl, NO_2)

Z = (Cl, Br)

Manuscript submitted for publication in:

Journal of Molecular Structure

Spectroscopic and Theoretical Studies of some 2-(2'-haloacetyl)-5-substituted: 1-Methylpyrrole, Furan and Thiophene

Contents: 23 pages, 11 tables, 7 figures, 2 schemes, 1 supplementary table and 1 supplementary note

***Corresponding authors:**

Jéssica Valença and **Daniel N.S. Rodrigues,**

Conformational Analysis and Electronic Interactions Laboratory, Instituto de Química, Universidade de São Paulo, P. O. Box 26077, 05513-970, São Paulo, SP, Brazil.

E-mail: jvalenca@iq.usp.br (J. Valença)

dannopper@gmail.com (D.N.S. Rodrigues)

Spectroscopic and Theoretical Studies of some 2-(2'-haloacetyl)-5-substituted: 1-Methylpyrrole, Furan and Thiophene

Jéssica Valença[a*], Daniel N. S. Rodrigues[a*], Paulo R. Olivato[a], Maurizio Dal Colle[b]

[a]*Conformational Analysis and Electronic Interactions Laboratory, Instituto de Química, USP, CP 26077, 05513-970, São Paulo, SP, Brazil*

[b]*Dipartimento di Scienze Chimiche e Farmaceutiche, Università di Ferrara,44121, Ferrara, Italy*

Abstract

The conformational study of some 2-(2'-haloacetyl)-5-substituted five-membered heteroaromatic compounds Z-$CH_2C(O)(C_4H_2X)$-Y bearing a halogen (Z = Cl or Br) at the 2'-position and (Y = NO_2, H, Me or Cl) substituents at the 5-position of the heteroaromatic ring for X = NMe, O and S was performed by IR carbonyl stretching band (ν_{CO}) analysis supported by the harmonic frequency, NBO and PCM calculations on the minima and saddle-point structures obtained at the M05-2X/aug-cc-pVTZ level. The computational results predicted the presence of four stable conformers, classified by the orientation of the X_{ring}–C–C=O (*syn*/*anti*) and the O=C–C–Z (*anticlinal*/ *synperiplanar*) moieties as *ac*(*syn*), *sp*(*syn*), *ac*(*anti*) and *sp*(*anti*). The *anti*/*syn* equilibrium controls the relative stabilities of the conformers to a large extent while the

anticlinal/*synperiplanar* accounts for the observed trend of the IR carbonyl band components. The computed ν_{CO} frequencies and the PCM trend of the relative abundance in solvents of increasing permittivity allowed the pairs of *ac*(*syn*)/*ac*(*anti*) and *sp*(*syn*)/*sp*(*anti*) conformers to be assigned to the lower and higher ν_{CO} frequency IR carbonyl doublet components, respectively. The PCM data failed to reproduce the experimental carbonyl triplet found in chloroform. However, the additional component could be justified by assuming the formation of complexes constituted by one chloroform molecule hydrogen bonded to the conformers in a PCM chloroform continuum.

The NBO and short contact analysis suggested that the *syn*/*anti* conformational equilibrium is governed mainly by electrostatic interactions, while the *anticlinal*/*synperiplanar* depends to different extents on both orbital and electrostatic interactions.

Keywords: Infrared spectroscopy; theoretical calculations; solvent effect; conformational analysis; 2-(2'-haloacetyl)-5-substituted heteroaromatic compounds.

1. Introduction

Aromatic heterocyclic compounds are widely studied from a synthetic point of view as building blocks [1,2], due to their applicability in the polymer [3,4] and food industries [5,6] and to their potential biological activity [7].

In 2-formylthiophene and some thiophene-2-carbonyl halides [8,9], the higher relative abundance of the *cis* conformer was ascribed to the coulombic interaction between the oppositely charged $O^{\delta-}_{(CO)}$ and $S^{\delta+}$ atoms. The same stability order for 2-acetylthiophene in *n*-hexane and benzene was determined through Kerr constants and dipole moments [10] and was confirmed by DFT calculations and infrared spectra in carbon tetrachloride and chloroform [11]. These findings are also supported by Photoelectron (PE) and Electron Transmission (ET) spectral analysis [12], as well as by *ab-initio* HF/6-31G** and MP2/6-31G** calculations [13]. Therefore, all these studies indicate that the *cis* conformer (relative to the O=C–C–S moiety) is more stable than the *trans*.

For 2-acetylfuran, the observed trend is reversed. The Kerr constants and dipole moments in *n*-hexane and benzene [10] indicate the *trans* conformer to be the more stable. An NMR, infrared and DTF study [14] also reported preference for the *trans* conformer in vacuum, dichloromethane and acetone. Semi-empirical calculations suggest that electronic delocalisation should favour the *cis* conformer, indicating that the *trans* preference is mainly a consequence of the strong Repulsive Field Effect (RFE) that acts on the $O^{\delta-}_{(CO)}\ldots O^{\delta-}$ short contact [15].

For 2-acetylpyrrole, the *cis* conformer is highly stabilised in CS_2/CD_2Cl, CCl_4, $CHCl_3$, CH_3CN and acetone-d6 by the intramolecular hydrogen bond $N–H^{\delta+}\ldots O^{\delta-}_{(CO)}$ [16]. In the same study, only this conformer was evidenced in *N*-methyl-2-acetylpyrrole.

In the solid state, *N*-methyl-2-trichloroacetylpyrrole assumes an *s-cis* conformation, which is stabilised by a network of intermolecular halogen and hydrogen bonding interactions [17]. DFT calculations assigned the singlet ν_{CO} IR symmetric band at 1681 cm^{-1} to this structure [18]. Similarly, the *s-cis* conformer was ascribed to the most intense doublet ν_{CO} component at a lower frequency (1662 cm^{-1}) for *N*-methyl-2-(2-chloroacetyl)pyrrole [19].

The present paper reports infrared and theoretical studies of some 2-(2'-haloacetyl)-5-substituted five-membered heteroaromatic compounds $Z–CH_2C(O)(C_4H_2X)–Y$ (**1**–**7**) bearing halogen (Z = Cl or Br) at the 2'-position and the substituent (Y = NO_2, H, Me or Cl) at the 5-position of the heteroaromatic ring, for X = NMe, O and S (See Scheme 1). These compounds were chosen taking into account that both the X and Y substituents may affect the *syn/anti* and the *synperiplanar*/*anticlinal* conformational equilibrium with respect to the X–C–C=O and O=C–C–Z moieties, respectively.

2. Experimental

2.1. Materials

All solvents for IR measurements were spectrograde and were used without further purification. The title compounds **1**–**7** were commercially available (**1**–**3** from Ablock Pharmatech and **4**–**7** from Sigma-Aldrich).

2.2. IR measurements

The IR spectra were recorded with a Michelson Bomem MB100 FTIR spectrometer, with 1.0 cm^{-1} resolution at a concentration of 1.0×10^{-2}mol dm^{-3} in *n*-hexane, carbon

tetrachloride, chloroform, dichloromethane and acetonitrile using a 0.519 mm sodium chloride cell, for the fundamental carbonyl region (1800–1600 cm^{-1}). The spectra of the carbonyl first overtone (3600–3100 cm^{-1}) were recorded in carbon tetrachloride solution (1.0×10^{-2}mol dm^{-3}), using a 1.00 cm quartz cell. The overlapping carbonyl bands (fundamental and first overtone) were resolved by means of the Grams/32 curve-fitting software, version 4.04, Level II [20]. This software detects, through the second derivative of the actual carbonyl band, the number of components that composes it and then, statistically, adjusts them to the original band using a Gaussian/Lorentzian profile. The conformer populations for compounds **1**–**7** in the referred solvents were expressed as percentages of the integrated intensity estimated from the integrated absorbance $B = \int_{band} \ln(I_o/I)_\nu \, d\nu$ (ν in cm^{-1}) for each resolved carbonyl multiplet (doublet, triplet or quartet) component, on the assumption of equal integrated molar absorption coefficient $\overline{A}$ [21] for all the conformers (for details see Table S1and Note S1).

2.3. Theoretical calculations

The local and global minima, as well as the first order saddle point geometries, were found by rotating the α (O=C–C–Z) and δ (X–C–C=O) dihedral angles, from 0º to 180º with steps of 10º, through the relaxed SCAN method (Mod Redundant) implemented in the Gaussian 09 package [22] at the M05-2X/aug-cc-pVDZ [23,24] level of theory. The final geometries, harmonic vibrational modes and orbital interaction at 298 K were refined at the same M05-2X/aug-cc-pVTZ [25] level. Condensed phase Polarisable Continuum Model (PCM) [26] calculations were carried out at the M05-2X/aug-cc-pVTZ level, as implemented in Gaussian 09, in order to obtain the Gibbs free energies of solvation. Relative energies were estimated using the harmonic zero point energy

(ZPE) correction. Due to the symmetry of the conformers, either C_1 or C_S point groups, in order to obtain accurate molar fractions, the thermodynamic probability factor ($\omega = e^{(S/R)}$) was applied as a weighting factor of 2 or 1, respectively. The NBO 3.1 program [27] implemented in the Gaussian 09 package was used to estimate delocalisation energies (E2) by means of second-order perturbation theory. The partial atomic charges were calculated using Natural Population Analysis (NPA) [27].

3. Results and Discussion

Table 1 collects the frequencies and relative intensities of the resolved components of the carbonyl stretching (ν_{CO}) band for compounds **1**–**7** in solvents of increasing relative permittivity, from *n*-hexane to acetonitrile [28]. In general, a doublet is observed, with a less intense component at higher ν_{CO} frequency (*ca.* 18 cm^{-1}). For all compounds, the relative intensity of this component increases as the dielectric constant of the medium increases. In chloroform, an additional ν_{CO} component at the lowest frequency is detected for compounds **1**, **3** and **5**. This triplet component is the most intense for compound **3** and least intense for compounds **1** and **5**.

In contrast, for compound **7** in *n*-hexane, the doublet is split into a quartet with a difference of *ca.* 20 cm^{-1} between the highest frequency (1702 cm^{-1}) and the third component (1683 cm^{-1}) and between the second component (1694 cm^{-1}) and that at the lowest frequency (1673 cm^{-1}). The solvent effect on the carbonyl band components is illustrated in Figures 1–3 for compounds **1**, **2** and **7**, taken as representatives of the 2-(2'-haloacetyl)-5-substituted 1-methylpyrrole (**1**), furans (**2**–**5**) and thiophenes (**6** and **7**). The carbonyl first overtone band profiles match those of the fundamentals. The resolved components, in carbon tetrachloride, appear at frequencies twice those of the fundamental minus two times the mechanical anharmonicity [21] of *ca.* 20 cm^{-1}. These

features indicate the existence of at least two conformers in solution for the studied compounds **1–7** [29,30], ruling out the existence of any vibrational effect in the fundamental transition of the ν_{CO} mode.

In Table 2, the relative energies and populations, dipole moments, carbonyl stretching frequencies and dihedral angles of the global and local minima at the M05-2X/aug-cc-pVTZ level of theory for compounds **1–7** are reported.

The calculation results suggest the presence in vacuum of four conformers, which may assume either an *anticlinal* or *synperiplanar* geometry on the α dihedral angle and either a *synperiplanar* or *antiperiplanar* geometry on the δ dihedral angle. Therefore we labelled the *anticlinal* and *synperiplanar* geometries of the α dihedral angle as *ac* and *sp*, respectively. As for the δ dihedral angle, the short terms *syn* and *anti* were used. Therefore, the four conformers in the present work are labelled as *ac*(*syn*), *sp*(*syn*), *ac*(*anti*) and *sp*(*anti*).

The α angle varies in the range 102–113º in the *ac* conformers, while assuming the value of exactly 0º, with the exception of compound **5** (5°), in the *sp* conformers. With regard to the *syn* and *anti* conformation, the corresponding δ angle values are close to or exactly equal to 0° or 180º. As a consequence, the *sp*(*syn*) and the *sp*(*anti*) conformers of all derivatives, except the *sp*(*syn*) of **5**, belong to the Cs point group due to the presence of a symmetry plane, while the *ac*(*syn*) and the *ac*(*anti*) conformers belongs to the C_1 point group. The four conformers of compound **3**, taken as representatives for the whole series, are illustrated in Figure 4.

For the methylpyrrole derivative **1**, the lowest frequency *ac*(*syn*) conformer is the most stable and the least polar, followed by the *sp*(*syn*) and by the two (*anti*) rotamers, both destabilised by more than 5.7 kcal mol^{-1}.

On the contrary, for all of the furan derivatives **2**–**5**, the lowest frequency *ac*(*anti*) conformer becomes the most stable, while the highest ν_{CO} frequency *sp*(*syn*) is the least stable. The relative stability of the *sp*(*anti*) and the *ac*(*syn*) conformers is likely to be affected by the nature of the Z and Y substituents. For instance, the *sp*(*anti*) conformers are destabilised to about the same extent in the **3**–**5** derivatives (Z = Br) with respect to compound **2** (Z = Cl). Furthermore, the relative abundance of the *ac*(*syn*) conformers is almost equivalent in compounds **2**-**4** (Y = H, Me) and decreases to a larger extent in compound **5** (Y = NO_2).

For thiophenes **6** and **7**, the most and least stable conformers are, respectively, the lowest frequency *ac*(*syn*) and the highest frequency *sp*(*anti*), as for compound **1**. In contrast to compound **1**, the *ac*(*anti*) conformers are significantly stabilised at energy values comparable with those of the *sp*(*syn*) conformers.

The computed ν_{CO} frequency differences on the *syn*/*anti* equilibrium are usually small for compounds **2**–**7**. On the contrary, for compounds **1**–**7**, the calculated ν_{CO} frequencies of the two *synperiplanar* conformers (*syn* and *anti*) are higher than those of the corresponding *anticlinal* conformers by *ca*. 20 cm^{-1}, which is in agreement with the observed ν_{CO} differences of the resolved IR doublet components.

In order to better understand the conformational preferences in the condensed phase for compounds **1**–**7**, the four conformers were fully optimised with PCM at the M05-2X/aug-cc-pVTZ level of theory. The results are summarised in Tables 3a and 3b.

For compound **1** the relative abundance of the higher frequency *sp*(*syn*) conformer in vacuum (16%) increases with respect to the most stable *ac*(*syn*) as the solvent polarity increases, up to 36% in the higher permittivity solvent, acetonitrile. This trend relatively closely matches the experimental results, which show a progressive intensity increase of the higher frequency carbonyl doublet component from 30% in *n*-hexane to 48% in

acetonitrile. Therefore, the computed higher frequency *sp*(*syn*) conformer can be unequivocally ascribed to the higher IR frequency carbonyl doublet component. A relevant mismatch between the calculated and experimental findings occurs in chloroform, as the experimental carbonyl band shows an additional third component at the lowest frequency. Literature data report that a conformer may be stabilised by intermolecular hydrogen bonding in chloroform [31,32]. Therefore, we tried to simulate the solvation effect in a PCM chloroform continuum at the M05-2X/aug-cc-pVTZ level on the complexes formed by a single chloroform molecule hydrogen bonded to the *sp*(*syn*) and *ac*(*syn*) conformers. The intermolecular hydrogen bonding interaction is depicted in Figure 5, while Table 4 collects the computed energies, the carbonyl frequencies, the orbital interactions and the relevant geometric parameters involving the interacting atoms on the complexes. Since the higher frequency *sp*(*syn*) conformer has a symmetry plane (C_S symmetry), the approach of the chloroform molecule to the carbonyl oxygen atom from either plane side leads to indistinguishable complexes (*complex 1*). At variance, with the lowest frequency *ac*(*syn*) conformer, two distinct stable complexes (*complex 2* and *complex 3*) can be obtained, whose frequencies differ by about 4.5 cm^{-1}. Although the relative abundances of the complexes calculated in vacuum and in the $CHCl_3$ continuum (PCM) are not quite accurate, these calculations predict three distinct components for the carbonyl band whose frequencies are in agreement with the experimental findings (Table 1).

It should be pointed out that the results presented in this paper disagree with the interpretations of Dubis et al. [19] (see Introduction), who assigned the higher frequency doublet component to the *s-trans* conformer [either *ac*(*anti*) or *sp*(*anti*)] in a *syn*/*anti* conformational equilibrium. On the contrary, the present results indicate that the two carbonyl components are related to the *synperiplanar*/*anticlinal* conformational

equilibrium. This behaviour is similar to that described for the doublet in the *n*-hexane IR spectra of the α-haloacetophenones Ph–C(O)CH_2–X (X = F, Cl, Br and I) [33] and is in line with the findings of Ducati et al. [16], who assert that only the *s-cis* conformer should be stable enough to be observed at room temperature.

Likewise, the experimental findings for the furan derivatives **2**–**5** in solution can be explained on the basis of the *synperiplanar*/*anticlinal* conformational equilibrium. The PCM calculations in *n*-hexane predict the same conformer stability order as found in the gas phase. However, the solvation affects the ν_{CO} frequencies of the four conformers and, in particular, decreases the energy difference between the two *anticlinal* (*syn* and *anti*) rotamers, as well as between the two *synperiplanar* (*syn* and *anti*) forms. With regard to the two *anticlinal* rotamers of compounds **2**–**5**, the mean frequency difference decreases progressively as the solvent dielectric constant increases, varying from about 5.8 cm^{-1} in vacuum to about 2.4 cm^{-1} in acetonitrile. Therefore, as the mean experimental Full Width at Half Maximum (FWHM) of the distinct band components varies from 11.7 to 18.3 cm^{-1} (see Table 1), the two *anticlinal* conformers should coalesce into a single unresolved peak at the low frequency side.

The same arguments hold for the *synperiplanar* (*syn* and *anti*) conformers of compounds **2**–**5**, in spite of the large frequency difference calculated for compound **5**. In that case, in fact, $\Delta\nu_{CO}$ varies from 17 cm^{-1} in vacuum to 14 cm^{-1} in n-hexane, CCl_4 and $CHCl_3$. However, as the corresponding relative abundance of the *sp*(*syn*) conformers is in the range 0–2%, the calculations still suggest the occurrence of a single peak at the high frequency side. The sum of the computed (PCM) relative populations of the two *anticlinal* conformers decreases with respect to the sum of the two *synperiplanar* forms as the permittivity of the solvent increases, going from a mean value of *ca*. 84% in *n*-hexane to *ca*. 65% in acetonitrile.

This trend agrees fairly well with the experimentally observed intensity decrease of the lowest frequency component of the carbonyl doublet on going from the lowest permittivity solvent, *n*-hexane (mean value *ca*. 80%), to the highest, acetonitrile (mean value *ca*. 61%). The carbonyl band for compounds **3** and **5** in chloroform shows three components that can be explained with the formation of complexes analogous to those described for compound **1**.

Following the same arguments, the PCM calculations suggest that the two pairs of *anticlinal* and *synperiplanar* conformers of compounds **6** and **7** behave in a similar way to the corresponding forms of the **2**–**5** derivatives. In fact, all of the relevant data, such as the $\Delta\nu$ for the *anticlinal* (and the *synperiplanar*) conformers, or the variation of the sum of the relative populations of the rotamers with the solvent permittivity, are comparable to those calculated for compounds **2**–**5**. Therefore, it can be inferred that the IR bands are likely to appear as a doublet and that the low frequency component can be assigned to the two *anticlinal* (*syn* and *anti*) conformers, with the exception of the band of compound **7**, in n-hexane, which can be resolved into four distinct components due to their narrower FWHM.

The potential energy surfaces (PES) of compounds **1**–**7** were obtained by varying the α and δ dihedral angles from 0º to 180º with a step size of 10º at the M05-2X/aug-cc-pVDZ level. Further optimisation was performed on the six saddle points detected. The saddle points were labelled with capital letters (*SP1-SP6*) in order to avoid confusion with orbital hybridisation. Their energies and geometries are reported in Table 5 for compounds **2** and **6**.

The interconversion path from *syn* to *anti* conformers requires the rotation of the X–C–C=O moiety through the high energy saddle points *SP2* and *SP4* (barriers of *ca*. 9.0 kcal mol^{-1}), whose geometries are characterised by the lack of conjugation between the

aromatic ring and the carbonyl group. At variance, the interconversion path from *anticlinal* to *synperiplanar* conformers involves the low energy saddle points *SP1* and *SP3* (barriers of *ca*. 2.1 kcal mol^{-1}), in which the Z–C–C=O moiety assumes a *synclinal* geometry (*ca*. 50º). The two dimensions PES for compounds **1**, **2** and **6**, taken as representatives of the series, are presented in Figure 6, while a diagram of the interconversion paths described is reported in Scheme 2 for compound **6**. The other two saddle points, *SP5* and *SP6* (barriers of *ca*. 4.1 kcal mol^{-1}), are both planar and transform the *anticlinal* conformers into their mirror images, which have the same properties as those previously presented in Table 2 for the *anticlinal* conformers. These interconversions through the α dihedral angle are shown in the one dimension PES in Figure 7.

To recognise the electrostatic interactions that contribute to the stabilisation of each conformer, some selected Natural Population Analysis (NPA) charges and interatomic distances are collected in Tables 6, 7a and 7b, respectively.

Both the *syn* and the *anti* conformers of compound **1** are destabilised by electrostatic repulsion between atoms separated by distances shorter than the sum of the van der Waals radii (ΣvdWr). These repulsions involve, for the *anti* conformers, the positively charged hydrogen atoms of the $N–CH_3$ and methylene groups and, for the *syn* forms, the negatively charged carbonyl oxygen and nitrogen atoms. On the contrary, only the *syn* conformers are stabilised by the short contact between the oppositely charged $H^{\delta+}_{NMe}$ and $O^{\delta-}_{CO}$ atoms. The two *synperiplanar* conformers, unlike the two *anticlinal* forms, exhibit the electrostatic destabilising interaction caused by the short contact between the negatively charged carbonyl oxygen and chlorine atoms. All these electrostatic interactions account for the major stability of the *syn* conformers with respect to the *anti* forms, as well as for the *anticlinal* preference over the *synperiplanar*.

For the furan derivatives **2**–**5**, the short contact $O^{\delta-}{}_{CO}\cdots H^{\delta+}{}_{12}$ interaction enhances the stabilisation of the two *anti* conformers, while the electrostatic repulsion between the negatively charged furan and carbonyl oxygen atoms destabilises the two *syn* forms. These interactions, and the absence of those involving one hydrogen atom of the N–Me group described for compound **1**, justify the preference for the *anti* conformers of the furan derivatives. This behaviour has been already reported for similar molecules [14, 15]. As for compound **1**, the Repulsive Field Effect [34] between the C=O…C–Z dipoles (Z = Cl or Br) accounts for the lowest stability of the *synperiplanar* (*anti*) and *synperiplanar* (*syn*) conformers with respect to the *anticlinal* (*anti*) and *anticlinal* (*syn*) forms, respectively.

For compounds **6** and **7**, the *syn* conformers are stabilised by the short contact electrostatic interactions that involve the oppositely charged $O^{\delta-}{}_{CO}$ and thiophene $S^{\delta+}$ atoms, while the *synperiplanar* conformations are destabilised by the Repulsive Field Effect previously described for the *synperiplanar* conformers of compounds **2**–**5**.

The natural bond orbital (NBO) analysis was performed for all compounds, to identify the relevant orbital interactions that contribute to the stabilisation of each conformer. Tables 8a and 8b show some selected orbital interactions and energies.

The heteroatom lone pair LP_X is delocalised to both the $\pi^*_{C(5)=C(6)}$ and $\pi^*_{C(7)=C(8)}$ orbitals. The mean values of the sum of the $LP_X \rightarrow \pi^*_{C(5)=C(6)}$ and $LP_X \rightarrow \pi^*_{C(7)=C(8)}$ delocalisation energies of all conformers bearing the same X heteroatom in the series **1**–**7** decrease progressively as the atomic number of the X ring atom increases, from *ca*. 54.4 kcal mol^{-1} for compound **1** (X = N) to 38.5 kcal mol^{-1} for compounds **2**–**5** (X = O) to 34.8 kcal mol^{-1} for compounds **6** and **7** (X = S). For compounds **2**–**7**, the sum of the two interactions slightly stabilises the *synperiplanar* conformers (mean value 0.5 kcal mol^{-1}) in the *syn* orientation and the *anticlinal* forms (1.3 kcal mol^{-1}) in the *anti*

orientation. In contrast, their sum plays a relevant role in the *syn*/*anti* equilibrium, favouring the *syn* conformers over the *anti* by a mean value of about 4.6 kcal mol^{-1}.

The $\pi_{C(5)=C(6)}$ ring orbital interacts with both the carbonyl $\pi^*_{C(2)=O(1)}$ and the ring $\pi^*_{C(7)=C(8)}$ orbitals. The latter interaction contributes, together with the $\pi_{C(7)=C(8)} \rightarrow \pi^*_{C(5)=C(6)}$, to the aromatic ring conjugation. The comparison between the delocalisation energies indicates that the $\pi_{C(5)=C(6)} \rightarrow \pi^*_{C(2)=O(1)}$ interactions generally exceed those of $\pi_{C(5)=C(6)} \rightarrow \pi^*_{C(7)=C(8)}$ by 1–10 kcal mol^{-1}, with the exception of all the conformers of the nitro-substituted compound **5** and the *ac*(*anti*) of compound **4**. In these cases, the $\pi_{C(5)=C(6)} \rightarrow \pi^*_{C(7)=C(8)}$ interaction also exceeds that of $\pi_{C(7)=C(8)} \rightarrow \pi^*_{C(5)=C(6)}$, and thus favours ring conjugation over carbonyl delocalisation to a large extent. With regard to the *anticlinal*/*synperiplanar* equilibrium for compounds **2**–**7**, the $\pi_{C(5)=C(6)} \rightarrow \pi^*_{C(2)=O(1)}$ carbonyl delocalisation favours, in the *syn* and *anti* orientations, the *anticlinal* conformers over the *synperiplanar* forms by a mean value of 1.7 kcal mol^{-1}. Analogously, the overall effect of the $\pi_{C(5)=C(6)} \rightarrow \pi^*_{C(7)=C(8)}$ and $\pi_{C(7)=C(8)} \rightarrow \pi^*_{C(5)=C(6)}$ ring interactions always stabilises the *anticlinal* conformers with respect to the *synperiplanar* forms by less than 1.0 kcal mol^{-1} (compounds **1**–**3**, **5**–**7**) and 4.8 kcal mol^{-1} (compound **4**).

Following the same arguments for the *syn*/*anti* equilibrium, the sum of the $\pi_{C(7)=C(8)} \rightarrow \pi^*_{C(5)=C(6)}$ and $\pi_{C(5)=C(6)} \rightarrow \pi^*_{C(7)=C(8)}$ ring interactions indicates the *anti* preference for both the *anticlinal* and the *synperiplanar* conformers (mean value 1.2 kcal mol^{-1}), except for the *sp*(*syn*) of compound **4**. On the contrary, the $\pi_{C(5)=C(6)} \rightarrow \pi^*_{C(2)=O(1)}$ delocalisation mainly stabilises the *syn* orientation by less than 1.0 kcal mol^{-1}, apart from the *sp*(*anti*) conformers of **2**–**4**. The overall effect of the three interactions indicates a general preference for the *anti* conformation (0.7 kcal mol^{-1}), except for compound **4**.

For compounds **1**–**7**, the charge transfer interaction $LP_{O(1)}\rightarrow\sigma^*_{X(9)-C(8)}$ stabilises exclusively the *syn* conformers (mean value 0.6 kcal mol^{-1}), while that of $LP_{O(1)}\rightarrow\sigma^*_{X(9)-C(5)}$ affects only the *anti* conformers by *ca*. 1.5 kcal mol^{-1}.

Regarding the $O_1{=}C_2{-}C_3{-}Z_4$ moiety, the through-bond coupling interactions [35] $LP_{O(1)}\rightarrow\sigma^*_{C(2)-C(3)}$ and $LP_{O(1)}\rightarrow\sigma^*_{C(2)-C(5)}$ stabilise to almost the same extent (*ca*. 3 kcal mol^{-1}) all the *sp(syn,anti)* conformers of compounds **1–7** over the corresponding *ac(syn, anti)* forms. Additionally, the *sp*(*syn*, *anti*) conformers are also favoured by the $LP_{Z(4)}\rightarrow\sigma^*_{C(2)-C(3)}$ charge transfer interaction (*ca*. 1.9 kcal mol^{-1}). It should be noted that, in the same moiety, the $LP_{Z(4)}\rightarrow\sigma^*_{C(2)-C(5)}$ interaction uniquely affects the *sp*(*syn*, *anti*) conformers by *ca*. 0.7 kcal mol^{-1}, while the $LP_{Z(4)}\rightarrow\pi^*_{C(2)=O(1)}$, $\sigma_{C(3)-Z(4)}\rightarrow\pi^*_{C(2)=O(1)}$ and $\pi_{C(2)=O(1)}\rightarrow\sigma^*_{C(3)-Z(4)}$ interactions favour only those of *ac*(*syn*, *anti*) (mean value of the sum about 12.1 kcal mol^{-1}). Moreover, the latter interactions stabilise the *ac*(*anti*) by about 2.2 kcal mol^{-1} more than the *ac*(*syn*). Finally, the $\sigma_{C(3)-Z(4)}\rightarrow\sigma^*_{C(2)-C(5)}$ interaction (mean value *ca*. 3.1 kcal mol^{-1}) occurs solely in the *sp*(*syn*) conformers.

As can be seen from Tables 8a and 8b, the sum of all of the cited orbital interactions reproduces exactly the stability order of the conformers for compounds **1**, **6** and **7** and the two more stable *ac*(*anti*) and *ac*(*syn*) forms of compound **4**, as well as the preference for *anticlinal* over *synperiplanar* for all compounds. On the contrary, for the furan derivatives **2**, **3** and **5**, these interactions favour the less stable *ac*(*syn*) and *sp*(*syn*) conformers with respect, respectively, to the more stable*ac*(*anti*) and *sp*(*anti*) forms.

4. Conclusions

The conformational preferences of some 2-(2'-haloacetyl)-5-substituted 5-membered heteroaromatic compounds $Z{-}CH_2C(O)(C_4H_2X){-}Y$ bearing a halogen (Z = Cl or Br) at

the 2'-position and substituents (Y = NO_2, H, Me or Cl) in the 5-position of the heteroaromatic ring (X = NMe, O and S) have been determined by ν_{CO} IR analysis and theoretical calculations at the M05-2X/aug-cc-pVTZ level. The relaxed PES reveals four stable conformers for all compounds, labelled as *ac*(*syn*), *sp*(*syn*), *ac*(*anti*) and *sp*(*anti*). Their relative stability is controlled to a large extent by the *anti*/*syn* equilibrium, related to the X_{ring}–C–C=O moiety. In fact, the gas phase is characterised by the prevalence of the *syn* conformers for compounds **1**, **6** and **7** and of the *anti* forms for compounds **2**–**5**. In particular, the *syn* conformers were detected exclusively for compound **1**. Although the carbonyl oxygen atom is involved in the main electrostatic interactions that determine the *syn* or *anti* orientation, the changes in the ν_{CO} frequencies of the *ac*(*syn*)/*ac*(*anti*) pair, as well as those of *sp*(*syn*)/*sp*(*anti*), are negligible. On the contrary, in the *anticlinal*/*synperiplanar* equilibrium, referred to as the O=C–C–Z moiety, for all compounds **1–7**, the *anticlinal* conformers are always favoured over the *synperiplanar*. The latter are destabilised mainly by the Repulsive Field Effect between the C=O…C–Z dipoles (Z = Cl or Br), which is also responsible for their ν_{CO} frequencies increasing by *ca*. 20 cm^{-1}. These findings are in line with the *cis*/*gauche* frequency differences previously reported for the α-haloacetophenones [33].

Taking into account the frequency difference and the FWHM of the IR doublet components, it is reasonable to ascribe both the *sp*(*syn*) and *sp*(*anti*) conformers to the high frequency IR component and both the *ac*(*syn*) and *ac*(*anti*) to the low frequency one. These assignments are supported by the four distinct components resolved in the IR spectrum of compound **7** in n-hexane, which can be assigned, in order of increasing frequency and decreasing abundance, to the *ac*(*syn*), *ac*(*anti*), *sp*(*syn*) and *sp*(*anti*) conformers. Moreover, the PCM data indicate that the relative stability of the lower frequency *ac*(*syn*) and *ac*(*anti*) conformer pair decreases as the dielectric constant of the

media increases, which is in agreement with the experimental findings for the IR analytically resolved bands. However, the PCM data mismatch the IR results for compounds **1**, **3** and **5** in $CHCl_3$. The PCM solvation model in fact predicts a carbonyl doublet, in contradiction to the experimental triplet. The additional third component has been explained by assuming the formation of complexes constituted by a single chloroform molecule hydrogen-bonded to the conformers. The calculations performed for compound **1** in the gas phase and in $CHCl_3$ continuum predicted three distinct complexes to be formed with the *sp*(*syn*) (one complex) and the *ac*(*syn*) (two complexes) conformers, whose ν_{CO} frequencies are in line with the experimental findings.

The interconversion path from the *syn* to the *anti* conformers involves high energy saddle points that exhibit the lack of conjugation between the aromatic ring and the carbonyl group. On the contrary, in the *anticlinal*/*synperiplanar* interconversion path, the energy barriers are lowered by the *synclinal* geometry of the Z–C–C=O moiety. An additional interconversion path occurs through a planar saddle point that converts one *anticlinal* conformer into its mirror image.

The aromatic ring conjugative interactions, as well as the charge transfer to the carbonyl group, favour the *syn* conformations for all compounds **1–7**. However, while the *syn* arrangements of compounds **1**, **6** and **7** are further stabilised by attractive electrostatic interactions, the short contact $O^{\delta-}{}_{CO}\cdots O^{\delta-}{}_{(9)}$ electrostatic repulsion, in conjunction with the short contact $O^{\delta-}{}_{CO}\cdots H^{\delta+}{}_{12}$ attractive interaction, dictate the *anti* orientation preference for the furan derivatives **2–5**. Finally, the $\sigma_{C(3)\text{-}Z(4)}\rightarrow\pi^*_{C(2)=O(1)}$, $\pi_{C(2)=O(1)}\rightarrow\sigma^*_{C(3)\text{-}Z(4)}$ and $LP_{Z(4)}\rightarrow\pi^*_{C(2)=O(1)}$ orbital interactions heavily stabilise the *anticlinal* conformers uniquely, while the $LP_{Z(4)}\rightarrow\sigma^*_{C(2)\text{-}C(3)}$ and $LP_{O(1)}\rightarrow\sigma^*_{C(2)\text{-}C(3)}$ charge transfer interactions favour the *synperiplanar* forms to a minor extent.

Acknowledgments

The authors thank the Fundação de Amparo à Pesquisa do Estado de São Paulo (FAPESP) and Conselho Nacional de Desenvolvimento Científico e Tecnológico (CNPq) for financial support for this research, fellowships for P.R.O. and for a scholarship to J.V. The authors also thank the Coordenação de Aperfeiçoamento de Pessoal de Nível Superior (CAPES) for a scholarship to D.N.S.R.

References

[1] S. T. Henriksen, U. S. Sørensen, Tetrahedron Lett. 47 (2006) 8251–8254.

[2] N. S. Kumar, A. K. Mohanakrishnan, Tetrahedron. 66 (2010) 5660–5670.

[3] S. A. Jenekhe, Macromolecules. 23 (1990) 2848–2854.

[4] M. S. Maynork, T. L. Nelson, C. O'Sullivan, J. Lavigne, Org. Lett. 9 (2007) 3217–3220.

[5] S. Mihara, H. Masuda, J. Agric, Food Chem. 36 (1988) 1242–1247.

[6] C. F. Hwang, W. E. Riha III, B. Jin, M. V. Karwe, T. G. Hartman, H. Daun, C. T. Ho, LebensmWiss Technol. 30 (1996) 411–416.

[7] A. M. Isloor, B. Kalluraya, K. S. Pai, Eur. J. Med. Chem. 45 (2010) 825–830.

[8] J. Kao, L. Radom, J. Am. Chem. Soc. 101 (1979) 311–318.

[9] D. J. Chadwick, J. Chambers, G. D. Meakins, R. L. Snowden, J. Chem. Soc. Perkin Trans. 2 (1976) 1–7.

[10] C. L. Cheng, I. G. John, G. L. D. Ritchie, P. Gore, P. Farnell, J. Chem. Soc. Perkin Trans. 2. (1975) 744–751.

[11] R. Rittner, L. C. Ducati, C. F. Tormena, B. C. Fiorin, C. B. Braga, Spectrochim. Acta A. 79 (2011) 1071–1076.

[12] M. Dal Colle, C. Cova, G. Distefano, D. Jones, A. Modelli, N. Comisso, J. Phys. Chem. A 79 (2011) 1071–1076.

[13] G. Distefano, M. De Palo, M. Dal Colle, M. Guerra, J. Mol. Struct. 455 (1998) 131–140.

[14] R. Rittner, L. C. Ducati, C. F. Tormena, R. A. Cormanich, B. C. Fiorin, C. B. Braga, R. J. Abraham, Spectrochim. Acta A. 103 (2013) 84–89.

[15] J. Capdevila, E. Canadell, J. Heterocycl. Chem. 18 (1980) 1055–1056.

[16] L. C. Ducati, C. B. Braga, R. Rittner, C. F. Tormena, Spectrochim. Acta A. 116 (2013) 197–203.

[17] E. Bilewicz, A. J. Rybarczyk-Pirek, A. T. Dubis, S. J. Grabowski, J. Mol. Struct. 829 (2007) 208–211.

[18] A. T. Dubis, M. Domagala, S. J. Grabovski, New. J. Chem. 34 (2010) 556–566.

[19] A. T. Dubis, J. Phys. Chem. Biophys. 4 (2014).

[20] Galactic Industries Corporation, Salem, NH, USA, 1991–1998.

[21] N. B. Colthup, L. H. Daly, S. E. Wiberly, Introduction to Infrared and Raman Spectroscopy, Academic Press, USA, 1990, 31–33.

[22] Gaussian 09, Revision D.01, M. J. Frisch, G. W. Trucks, H. B. Schlegel, G. E.Scuseria, M. A. Robb, J. R. Cheeseman, G. Scalmani, V. Barone, B. Mennucci, G. A. Petersson, H. Nakatsuji, M. Caricato, X. Li, H. P. Hratchian, A. F.Izmaylov, J. Bloino, G. Zheng, J. L.Sonnenberg, M. Hada, M. Ehara, K. Toyota, R. Fukuda, J. Hasegawa, M. Ishida, T. Nakajima, Y. Honda, O. Kitao, H. Nakai, T. Vreven, J. A. Montgomery Jr. , J. E. Peralta, F.Ogliaro, M. Bearpark, J. J. Heyd, E. Brothers, K. N. Kudin, V. N. Staroverov, R. Kobayashi, J. Normand, K. Raghavachari, A. Rendell, J. C. Burant, S. S.

Iyengar, J. Tomasi, M.Cossi, N. Rega, M. J. Millam, M. Klene, J. E.Knox, J. B. Cross, V. Bakken, C. Adamo, J. Jaramillo, R. Gomperts, R. E. Stratmann, O. Yazyev, A. J. Austin, R. Cammi, C. Pomelli, J. W. Ochterski, R. L. Martin, K. Morokuma, V. G. Zakrzewski, G. A. Voth, P. Salvador, J. J. Dannenberg, S. Dapprich, A. D. Daniels, Ö. Farkas, J. B. Foresman, J. V. Ortiz, J. Cioslowski, D. J. Fox, Gaussian, Inc., Wallingford CT, 2009.

[23] Y. Zhao, N. E. Schultz, D. G. Truhlar, J. Chem. Theory Comput. 2 (2006) 364–382.

[24] R. A. Kendall, T. H. Dunning Jr, R. J. Harrison, J. Chem. Phys. 96 (1992) 6796–6806.

[25] T. H. Dunning Jr., J. Chem. Phys. 90 (1989) 1007–1023.

[26] J. Tomasi, B. Mennucci, R. Cammi, Chem. Rev.105 (2005) 2999–3093.

[27] A. E. Reed, F. Weinhold. J. Chem. Phys. 83 (1985) 1736–1740.

[28] D. R. Lide (Ed.), CRC Handbook of Chemistry and Physics, CRC Press, Boca Raton, FL, 2005.

[29] P. R. Olivato, R. Rittner, Rev. Heteroatom Chem. 15 (1996) 115–159.

[30] A.Gaset, L. Lafaille, A.Verdier, A. Lattes, Bull. Soc. Chim. Fr. 10 (1968) 4108–4112.

[31] K. B. Whetsel, R. E. Kagarise, Spectrochim. Acta. 18 (1962) 329–339.

[32] R. E. Kagarise, K. B. Whetsel, Spectrochim. Acta. 18 (1962) 341–352.

[33] P. R. Olivato, Guerrero, S. A. Y. Hase, R. Rittner, J. Chem. Soc. Perkin. Trans. 2 (1990) 465–471.

[34] L. J. Bellamy, Advances in Infrared Group Frequencies, Chapman and Hall, London, 1975.

[35] C.C. Levin, R. Hoffmann, W. J. Hehre, J. Hudec, J. Chem. Soc. Perkin 2 (1973) 210–220.

Figure and Scheme Captions

Fig. 1. IR spectra of 2-(-2'-chloroacetyl)-1-methylpyrrole (**1**) showing the carbonyl stretching band in *n*-hexane (a), carbon tetrachloride [fundamental (b) and first overtone (c)], chloroform (d), dichloromethane (e) and acetonitrile (f). The red line is the experimental band; the blue line is the fitted band; the black lines are the band components.

Fig. 2. IR spectra of 2-(2'-chloroacetyl)furan (**2**) showing the carbonyl stretching band in n-hexane (a), carbon tetrachloride [fundamental (b) and first overtone (c)], chloroform (d), dichloromethane (e) and acetonitrile (f). The red line is the experimental band; the blue line is the fitted band; the black lines are the band components.

Fig. 3. IR spectra of 2'(-2-bromoacetyl)-5-chlorothiophene (**7**) showing the carbonyl stretching band in *n*-hexane (a), carbon tetrachloride [fundamental (b) and first overtone (c)], chloroform (d), dichloromethane (e) and acetonitrile (f). The red line is the experimental band; the blue line is the fitted band; the black lines are the band components.

Fig 4. *sp*(*syn*) (a), *ac*(*syn*) (b), *sp*(*anti*) (c) and *ac*(*anti*) (d) conformers of 2-(2'-bromoacetyl)furan (**3**) optimised at the M05-2x/aug-cc-pVTZ level.

Fig. 5. Structures of the hydrogen bonding complexes between 2-(2'-chloroacetyl)-pyrrole and chloroform obtained at the M05-2x/aug-cc-pVDZ level: *Complex 1* [*sp*(*syn*)…$HCCl_3$]; *Complex 2* [*ac*(*syn*)…$HCCl_3$]; *Complex 3* [*ac*(*syn*)…$HCCl_3$].

Fig. 6. Potential energy surfaces of compounds **1**, **2** and **6** obtained at the M05-2x/aug-cc-pVDZ level.

Fig. 7. One dimension potential energy surfaces of the α dihedral angle for compound **2** when δ dihedral angle is 0º (black line) or 180º (red line).

Scheme 1. Atom labelling of 2-(2'-haloacetyl)-5-substituted five-membered heteroaromatic compounds Z–$CH_2C(O)(C_4H_2X)$–Y (**1–7**) and definition of the relevant dihedral angles.

Scheme 2. Interconversion of the four conformers of 2-(-2'-bromoacetyl)thiophene. All energy values are in kcal mol^{-1}. $E_{(Rel)}$ indicates the energy relative to the minimum energy structure *ac*(*syn*). ΔE refers to the proper energy difference between two conformers. ΔE* refers to the energy difference between a minimum structure and that of a saddle point (*SP*).

Table 1

Frequencies (ν, cm^{-1}), integrated absorbances (B, cm^{-1}) and relative intensities of the carbonyl stretching band components in the IR Spectra of 2-(2'-haloacetyl)-5-substituted five-membered heteroaromatic compounds $ZCH_2C(O)(C_4H_2X)Y$ (**1**-**6**).

Comp	X	Y	Z	*n*-C_6H_{14} (ε=1.9)				CCl_4(ε=2.2)								$CHCl_3$(ε=4.8)				CH_2Cl_2(ε=9.1)				CH_3CN (ε=38)			
				ν	***P***[a]	HW[b]	B[c]	*ν*	*P*	HW	B	*ν*[d]	*P*	HW	B	*ν*	*P*	HW	B	*ν*	*P*	HW	B	*ν*	*P*	HW	B
1	NMe	H	Cl	1685	30	14.7	4.18	1680	26	15.0	3.53	3342	34	31.7	0.43	1672	29	18.9	5.89	1672	37	17.8	5.95	1673	48	15.8	5.49
				1664	70	10.5	9.53	1659	74	12.9	9.88	3299	66	32.1	0.82	1655	53	22.8	10.77	1654	63	20.9	9.99	1655	52	17.4	5.97
				-[e]				-				-				1641	18	19.7	3.74	-				-			
2	O	H	Cl	1713	40	13.4	2.88	1707	37	12.5	3.01	3393	47	27.8	0.98	1696	51	20.0	6.89	1697	56	16.4	4.95	1697	63	15.6	4.87
				1693	60	10.7	4.35	1688	63	12.9	5.07	3356	53	26.2	1.12	1679	49	21.9	6.50	1681	44	17.2	3.82	1682	37	14.3	2.88
3	O	H	Br	1709	14	9.4	1.49	1705	17	8.9	1.11	3382	18	33.6	0.51	1697	14	15.4	1.45	1692	37	18.5	2.70	1693	33	15.8	2.75
				1691	86	8.7	9.39	1686	83	13.8	5.42	3348	82	28.9	2.25	1684	33	16.9	3.57	1677	74	19.6	7.43	1678	68	16.3	5.68
				-				-				-				1672	53	18.4	5.74	-				-			
4	O	Me	Br	1700	16	14.9	1.64	1691	26	21.2	2.61	3367	23	31.3	0.42	1682	25	21.7	2.70	1683	35	20.0	4.55	1684	30	18.6	5.57
				1683	84	14.4	9.12	1675	74	14.6	7.32	3333	77	27.9	1.40	1665	75	21.0	8.03	1667	65	16.3	8.58	1669	70	14.6	12.70
5	O	NO_2	Br	1718	9	8.7	0.18	1715	14	10.9	0.92	3408	16	26.8	0.29	1712	21	12.8	1.38	1712	17	10.7	0.55	1711	33	13.7	0.76
				1702	91	13.3	1.76	1698	86	15.8	5.87	3375	83	28.4	1.52	1697	57	14.8	3.66	1695	83	14.5	2.77	1695	67	14.9	1.54
				-				-				-				1687	22	18.6	1.43	-				-			
6	S	H	Br	1695	16	13.0	2.56	1690	17	15.0	1.53	3364	16	29.7	1.05	1682	17	18.4	4.64	1681	30	18.7	4.22	1682	46	16.2	4.96
				1675	84	11.4	12.82	1670	83	12.6	7.53	3322	84	26.1	5.50	1663	83	18.7	23.16	1663	70	14.0	9.60	1664	54	12.3	5.70
7	S	Cl	Br	1702	3	11.8	0.39	-				-				-				-				-			
				1694	7	11.9	1.12	1687	16	17.5	2.59	3359	13	30.9	0.66	1682	17	18.9	2.52	1680	30	19.3	5.77	1681	33	16.6	7.36
				1683	6	8.5	0.87	-				-				-				-				-			
				1673	84	9.5	12.79	1668	84	12.5	13.65	3319	87	27.7	4.78	1663	83	19.4	12.50	1663	70	14.5	13.69	1665	67	12.9	14.71

ε = Relative permittivity

[a] Relative intensity of each component of the carbonyl stretching band expressed in percentage of the integrated absorbance.

[b] Full width at the half maximum (FWHM).

[c] Integrated absorbance.

[d] First overtone.

[e] Undetected component.

Table 2

Relativeenergies (E, kcal mol^{-1}), dipole moments (μ, D), selected dihedral angles (°) and the carbonyl IR stretching frequencies (ν, cm^{-1})for the minimum energy conformations of 2-(2'-haloacetyl)-5-substituted five-membered heteroaromatic compounds at M05-2x/aug-cc-pVTZ level.

Comp.	X	Y	Z	Conf.[a]	E[b]	ω[c]	P[d]	μ	ν	Dihedral Angles[e]	
										α	δ
1	NMe	H	Cl	*ac(syn)*	0	2	84	2.9	1762.7	106	-2
				sp(syn)	0.59	1	16	4.1	1789.6	0	0
				ac(anti)	5.70	2	0	4.6	1768.6	110	168
				sp(anti)	7.59	1	0	6.0	1793.9	0	180
2	O	H	Cl	*ac(syn)*	1.00	2	12	3.8	1808.2	113	-1
				sp(syn)	2.03	1	1	5.5	1830.5	0	0
				ac(anti)	0	2	64	3.5	1807.9	106	174
				sp(anti)	0.19	1	23	5.0	1827.6	0	180
3	O	H	Br	*ac(syn)*	1.20	2	11	4.0	1811.4	105	0
				sp(syn)	2.82	1	1	5.4	1826.7	0	0
				ac(anti)	0	2	81	3.6	1806.0	102	175
				sp(anti)	1.01	1	7	5.0	1821.2	0	180
4	O	Me	Br	*ac(syn)*	1.01	2	14	4.2	1801.6	106	-1
				sp(syn)	2.65	1	1	5.7	1825.3	0	0
				ac(anti)	0	2	79	4.4	1792.5	102	176
				sp(anti)	1.10	1	6	5.8	1818.9	0	180
5	O	NO_2	Br	*ac(syn)*	2.00	2	3	5.9	1830.8	109	0
				sp(syn)	4.03	1	0	6.2	1855.2	5	1
				ac(anti)	0.00	2	90	2.3	1822.6	103	173
				sp(anti)	1.13	1	7	2.1	1838.2	0	180
6	S	H	Br	*ac(syn)*	0	2	79	3.6	1788.6	105	0
				sp(syn)	1.25	1	5	5.1	1809.4	0	0
				ac(anti)	0.99	2	14	3.3	1790.7	103	180
				sp(anti)	1.89	1	2	4.8	1819.1	0	180
7	S	Cl	Br	*ac(syn)*	0	2	83	3.3	1789.9	107	0
				sp(syn)	1.31	1	5	4.5	1809.9	0	0
				ac(anti)	1.19	2	11	2.1	1794.4	105	180
				sp(anti)	2.25	1	1	3.5	1822.0	0	180

[a] Conformer assignment.The symbols ***ac*** and ***sp*** refers to *anticlinal* and *syn periplanar* geometries respectively on the Z-CH_2-C=O moiety in order to avoid confusion with the (***syn***) and (***anti***) symbols which refers to the *syn periplanar* and *anti periplanar* geometries respectively on the X-C-C=O moiety.

[b] Harmonic ZPE corrected relative energies at 298 K.

[c] Thermodynamic probability factor. $\omega = e^{(S/R)}$

[d] Molar fraction in percentage.

[e] See scheme 1.

Table 3a

Relative energies (E, kcal mol^{-1}) and carbonyl stretching frequencies (ν, cm^{-1}) for compounds **1**, **6** and **7**in condensed phase at M05-2x/aug-cc-pVTZ level through PCM solvation model.

Comp.	X	Y	Z	Conf.[a]	*n*-C_6H_{14}			CCl_4			$CHCl_3$			CH_2Cl_2			CH_3CN		
					E [b]	*P*[c]	*v*	E	*P*	*v*	E	*P*	*v*	E	*P*	*v*	E	*P*	*v*
1	NMe	H	Cl	*ac(syn)*	0	84	1750.1	0	83	1747.4	0	74	1735.0	0.00	69	1729.2	0.07	64	1722.0
				sp(syn)	0.58	16	1775.1	0.51	17	1771.9	0.22	26	1758.7	0.07	31	1751.6	0	36	1743.7
				ac(anti)	5.08	0	1751.9	4.98	0	1748.3	4.62	0	1735.2	4.41	0	1727.8	4.06	0	1720.0
				sp(anti)	6.21	0	1772.8	5.97	0	1769.5	5.01	0	1755.2	4.49	0	1755.2	4.29	0	1743.2
6	S	H	Br	*ac(syn)*	0	75	1773.3	0	74	1770.1	0	67	1757.4	0	62	1749.9	0.09	56	1742.4
				sp(syn)	0.83	9	1794.2	0.74	11	1790.9	0.36	19	1777.5	0.13	25	1769.9	0	32	1762.1
				ac(anti)	1.02	13	1776.2	1.04	12	1773.1	1.10	10	1761.0	1.12	9	1754.1	1.22	8	1747.0
				sp(anti)	1.62	3	1802.6	1.56	3	1798.9	1.34	4	1786.8	1.22	4	1779.3	1.20	4	1771.6
7	S	Cl	Br	*ac(syn)*	0	80	1775.7	0	79	1772.6	0	72	1760.2	0	66	1753.0	0.06	59	1745.5
				sp(syn)	0.92	9	1794.8	0.82	10	1791.6	0.41	18	1778.6	0.17	25	1771.3	0	33	1763.9
				ac(anti)	1.25	10	1779.5	1.26	9	1777.4	1.31	8	1765.6	1.34	6	1758.9	1.46	5	1752.2
				sp(anti)	1.96	1	1806.7	1.90	2	1803.5	1.64	2	1790.9	1.51	3	1783.7	1.45	3	1776.4

[a] Conformer assignment.

[b] Harmonic ZPE corrected relative energies.

[c] Molar fraction in percentage.

Table 3b

Relative energies (kcal mol^{-1}) and carbonyl stretching frequencies (cm^{-1}) for compounds **2-5** in condensed phase at M05-2x/aug-cc-pVTZ level through PCM solvation model.

Comp.	X	Y	Z	Conf.[a]	*n*-C_6H_{14}			CCl_4			$CHCl_3$			CH_2Cl_2			CH_3CN		
					E [b]	*P*[c]	*v*	E	*P*	*v*	E	*P*	*v*	E	*P*	*v*	E	*P*	*v*
2	O	H	Cl	*ac(syn)*	0.84	15	1793.8	0.83	16	1790.8	0.76	21	1777.9	0.70	23	1770.1	0.63	24	1762.1
				sp(syn)	1.37	3	1813.6	1.26	4	1809.9	0.78	10	1794.6	0.48	16	1785.8	0.18	25	1777.1
				ac(anti)	0.13	51	1792.5	0.20	47	1789.3	0.49	32	1776.9	0.66	24	1770.2	0.81	17	1763.7
				sp(anti)	0	31	1812.4	0	33	1809.9	0	37	1795.9	0	37	1787.8	0	34	1780.0
3	O	H	Br	*ac(syn)*	0.85	17	1795.0	0.77	19	1791.5	0.41	28	1776.7	0.17	34	1767.6	0	40	1760.4
				sp(syn)	2.07	1	1810.3	1.89	1	1807.7	1.16	4	1791.8	0.72	7	1783.3	1.48	11	1774.4
				ac(anti)	0	72	1790.8	0.00	69	1788.0	0	55	1775.5	0	45	1768.7	0.20	35	1761.9
				sp(anti)	0.73	10	1806.9	0.66	11	1805.0	0.41	14	1791.1	0.27	14	1783.8	0.08	14	1776.4
4	O	Me	Br	*ac(syn)*	0.70	21	1784.3	0.62	23	1781.6	0.24	34	1764.6	0	40	1754.9	0.25	31	1745.3
				sp(syn)	1.93	1	1805.3	1.77	2	1800.8	1.07	4	1784.9	0.66	7	1775.1	0.49	10	1765.1
				ac(anti)	0	69	1776.7	0	66	1773.4	0	51	1760.4	0	40	1753.1	0	47	1745.8
				sp(anti)	0.81	9	1801.4	0.74	9	1797.7	0.47	11	1783.0	0.33	13	1774.7	0.43	12	1766.3
5	O	NO_2	Br	*ac(syn)*	1.61	6	1819.7	1.50	7	1817.1	0.12	13	1806.7	0.65	20	1800.1	0.12	24	1800.1
				sp(syn)	3.10	0	1843.4	2.86	0	1841.7	0.46	2	1829.3	1.20	4	1823.6	0.46	9	1823.2
				ac(anti)	0	84	1813.3	0	82	1811.3	0	70	1804.2	0	59	1800.3	0	42	1805.9
				sp(anti)	0.85	10	1829.2	0.78	11	1827.1	0.20	15	1819.1	0.33	17	1815.0	0.20	15	1819.8

[a] Conformer assignment.

[b] Harmonic ZPE corrected relative energies.

[c] Molar fraction in percentage.

Table 4

Relative energies (kcal.mol^{-1}), selected interatomic distances (Å), selected angles (deg), carbonyl stretching frequencies (cm^{-1}), selected NBO interactions (kcal.mol^{-1}) for the minimum energy conformations of 2-(2'-chloroacetyl)-1-methylpyrrole **1** at M05-2x/aug-cc-pVDZ level.

Complexes	Gas Phase			PCM ($CHCl_3$)			NPA Charges		NBO interactions[a]			Interatomic distance and angle		
	E[a]	P[b]	ν_{CO}	E	P	ν_{CO}	$O_{(1)}$	$H_{(CHCl3)}$	$LP_{O1}\rightarrow\sigma_{HC}$[c]	$LP_{O1}\rightarrow\sigma_{HC}$[d]	$\pi_{CO}\rightarrow\sigma_{HC}$	$O_{(1)}...H$[e]	Δl[f,g]	∠O...H-C
Complex 1[h]	0	69	1771.8	0	74	1764.9	-0.619	0.293	1.92	1.16	0.75	2.19	-0.53	132.6
Complex 2[i]	0.56	26	1747.3	0.67	23	1737.5	-0.632	0.284	1.97	0.08	2.07	2.20	-0.52	148.3
Complex 3[j]	1.55	5	1753.9	1.96	3	1742.0	-0.642	0.296	5.62	0.36	0.06	2.08	-0.64	155.1

[a] Relative energy valueof the charge transfer interaction between $O_{(CO)}\ldots H_{(CHCl3)}$.

[b] Relative population as percentage.

[c] sp character lone pair.

[d] p character lone pair.

[e] Interatomic distance.

[f] Difference between the interatomic distance and the sum of van der Waals radii (ΣvdWr).

[g] ΣvdWr = 2.72 Å.

[h] Refers to: *sp*(*syn*)…$HCCl_3$.

[i] Refers to: *ac*(*syn*)…$HCCl_3$.

[j] Refersto: *ac*(*syn*)…$HCCl_3$.

Table 5

Relative energy (E, kcal.mol^{-1}), dipole moments (μ, D), selected dihedral angles (deg), for the first order saddle pointsconformations of 2-(2'-haloacetyl)-5-substituted five-membered heteroaromatic compounds (**2**, **6**) at M05-2x/aug-cc-pVTZ level.

Comp.	X	Y	Z	*SP*[a]	E[b]	μ	Dihedral Angles[c]	
							α	**δ**
2	O	H	Cl	*SP1*	2.82	5.2	53.2	2.4
				SP2	9.22	4.5	-0.4	87.3
				SP3	1.50	4.7	53.0	-179.1
				SP4	9.58	2.5	115.8	86.6
				SP5	3.33	2.7	180	0
				SP6	4.44	2.4	180	180
6	S	H	Br	*SP1*	2.21	4.9	46.6	1.7
				SP2	8.69	4.4	0.5	91.3
				SP3	2.89	4.6	47.8	-177.8
				SP4	8.50	2.3	107.8	89.7
				SP5	4.21	2.3	180	0
				SP6	4.51	2.1	180	180

[a] *SP* refers to saddle point.
[b] Energy difference between each saddle point and the minimum energy conformer of each compound.
[c] See scheme 1.

Table 6

NPA charges (e) at selected atomsfor the minimum energy conformations of 2-(2'-haloacetyl)-5-substituted five membered heteroaromatic compounds (**1**-**7**) at M05-2x/aug-cc-pVTZ level.

Comp.	X	Y	Z	Conf.	NPA Charges					
					O(1)	X(9)	H(12)	H(16/17/18)[a]	Z(4)	H(11/10)[b]
1	NMe	H	Cl	*ac(syn)*	-0.591	-0.389	0.239	0.235	-0.062	0.256
				sp(syn)	-0.579	-0.388	0.236	0.236	-0.045	0.251
				ac(anti)	-0.571	-0.406	0.252	0.217	-0.571	0.234
				sp(anti)	-0.563	-0.410	0.254	0.219	-0.038	0.243
2	O	H	Cl	*ac(syn)*	-0.522	-0.394	0.240	---	-0.050	0.238
				sp(syn)	-0.511	-0.392	0.234	---	-0.019	0.233
				ac(anti)	-0.537	-0.420	0.248	---	-0.044	0.235
				sp(anti)	-0.527	-0.428	0.249	---	-0.024	0.238
3	O	H	Br	*ac(syn)*	-0.523	-0.393	0.238	---	0.008	0.243
				sp(syn)	-0.512	-0.392	0.235	---	0.034	0.239
				ac(anti)	-0.538	-0.422	0.248	---	0.013	0.240
				sp(anti)	-0.528	-0.428	0.250	---	0.029	0.244
4	O	Me	Br	*ac(syn)*	-0.531	-0.413	0.236	---	0.005	0.243
				sp(syn)	-0.519	-0.411	0.233	---	0.030	0.238
				ac(anti)	-0.545	-0.442	0.247	---	0.010	0.240
				sp(anti)	-0.533	-0.441	0.248	---	0.025	0.243
5	O	NO_2	Br	*ac(syn)*	-0.495	-0.363	0.248	---	0.021	0.248
				sp(syn)	-0.486	-0.361	0.244	---	0.049	0.240
				ac(anti)	-0.516	-0.390	0.257	---	0.030	0.245
				sp(anti)	-0.506	-0.395	0.259	---	0.043	0.250
6	S	H	Br	*ac(syn)*	-0.547	0.537	0.232	---	0.009	0.244
				sp(syn)	-0.535	0.542	0.229	---	0.032	0.240
				ac(anti)	-0.545	0.495	0.247	---	0.013	0.243
				sp(anti)	-0.533	0.478	0.249	---	0.034	0.242
7	S	Cl	Br	*ac(syn)*	-0.546	0.560	0.236	---	0.012	0.245
				sp(syn)	-0.535	0.565	0.232	---	0.035	0.241
				ac(anti)	-0.543	0.520	0.250	---	0.016	0.245
				sp(anti)	-0.531	0.502	0.251	---	0.038	0.243

[a] Refers to the closest methyl hydrogen atom to the O(1) or H(10 or 11) atoms.
[b] Refers to the closest methylene hydrogen atom to theO(1) or H(16, 17 or 18) atoms.

Table 7a

Selected interatomic distances (Å) for the minimum energy conformations of 2-(2'-chloroacetyl)-1-methylpyrrole (**1**) at M05-2x/aug-cc-pVTZ level.

Comp.	X	Y	Z	Conf.	Interatomicdistances									
					$O_{(1)}...N_{(9)}$[a]	Δl[b,c]	$O_{(1)}...H_{(12)}$	Δl[d]	$O_{(1)}...Z_{(4)}$	Δl[e]	$O_{(1)}...H_{(16/17/18)}$	Δl	$H_{(16/17/18)}...H_{(10/11)}$	Δl[f]
1	NMe	H	Cl	*ac(syn)*	2.88	-0.19	>4	---	3.51	0.24	2.61	-0.11	>4	---
				sp(syn)	2.87	-0.20	>4	---	2.91	-0.36	2.60	-0.12	>4	---
				ac(anti)	>4	---	2.68	-0.04	3.53	0.16	>4	---	2.27	-0.13
				sp(anti)	>4	---	2.63	-0.09	2.88	-0.49	>4	---	2.18	-0.22

[a] Interatomic distances.

[b] Difference between the non-bonded atoms distances and the sum of van der Waals radii (ΣvdWr).

[c] ΣvdWr = 3.07 Å (N…O).

[d] ΣvdWr = 2.72 Å

[e] ΣvdWr = 3.27 Å (Cl…O).

[f] ΣvdWr = 2.40 Å (H…H)

Table 7b

Selected interatomic distances (Å) for the minimum energy conformations of 2-(2'-haloacetyl)-5-substituted five-membered heteroaromatic compounds (**2**-**7**) at M05-2x/aug-cc-pVTZ level.

Comp.	X	Y	Z	Conf.	Interatomic distances					
					$O_{(1)}...X_{(9)}$ [a]	Δl [b,c]	$O_{(1)}...H_{(12)}$	Δl [d]	$O_{(1)}...Z_{(4)}$	Δl [e]
2	O	H	Cl	*ac(syn)*	2.75	-0.29	>4	---	3.59	0.32
				sp(syn)	2.74	-0.30	>4	---	2.92	-0.35
				ac(anti)	>4	---	2.92	-0.20	3.50	0.23
				sp(anti)	>4	---	2.90	-0.18	2.93	-0.34
3	O	H	Br	*ac(syn)*	2.74	-0.30	>4	---	3.63	0.26
				sp(syn)	2.75	-0.29	>4	---	3.04	-0.33
				ac(anti)	>4	---	2.91	-0.19	3.58	0.21
				sp(anti)	>4	---	2.90	-0.18	3.04	-0.33
4	O	Me	Br	*ac(syn)*	2.75	-0.29	>4	---	3.64	0.27
				sp(syn)	2.74	-0.30	>4	---	3.04	-0.33
				ac(anti)	>4	---	2.91	-0.19	3.58	0.21
				sp(anti)	>4	---	2.90	-0.18	3.03	-0.34
5	O	NO_2	Br	*ac(syn)*	2.72	-0.32	>4	---	3.66	0.29
				sp(syn)	2.72	-0.32	>4	---	3.04	-0.33
				ac(anti)	>4	---	2.90	-0.18	3.57	0.20
				sp(anti)	>4	---	2.82	-0.10	3.05	-0.32
6	S	H	Br	*ac(syn)*	2.96	-0.36	>4	---	3.63	0.26
				sp(syn)	2.97	-0.35	>4	---	3.03	-0.34
				ac(anti)	>4	---	2.67	-0.05	3.59	0.22
				sp(anti)	>4	---	2.67	-0.05	3.03	-0.34
7	S	Cl	Br	*ac(syn)*	2.96	-0.36	>4	---	3.63	0.26
				sp(syn)	2.95	-0.37	>4	---	3.03	-0.34
				ac(anti)	>4	---	2.66	-0.06	3.61	0.24
				sp(anti)	>4	---	2.66	-0.06	3.03	-0.34

[a] Interatomic distances.

[b] Difference between the non-bonded atoms distances and the sum of van der Waals radii (ΣvdWr).

[c] ΣvdWr = 3.04 Å (O…O) and 3.32 Å (O…S).

[d] ΣvdWr = 2.72 Å.

[e] ΣvdWr = 3.27 Å (Cl…O) and 3.37 Å (Br…O).

Table 8a

Selected NBO interaction energies (kcal. mol^{-1}) for compounds **1**, **6** and **7** calculated at M05-2X/aug-cc-pVTZ level.

Orbitals	X=NMe, Y=H, Z=Cl (**1**)		X=S, Y=H, Z=Br (**6**)				X=S, Y=Cl, Z=Br (**7**)			
	ac(syn)	*sp(syn)*	*ac(syn)*	*sp(syn)*	*ac(anti)*	*sp(anti)*	*ac(syn)*	*sp(syn)*	*ac(anti)*	*sp(anti)*
$LP_{X9(p)} \rightarrow \pi^*_{C7=C8}$	59.3	58.4	38.0	37.9	36.3	35.2	38.9	38.8	37.1	36.0
$LP_{X9(p)} \rightarrow \pi^*_{C5=C6}$	49.4	50.6	33.8	34.5	32.1	31.7	32.1	32.9	30.6	30.1
$\pi_{C7=C8} \rightarrow \pi^*_{C5=C6}$	33.1	32.3	24.9	24.6	25.1	24.8	22.8	22.6	23.1	22.8
$\pi_{C5=C6} \rightarrow \pi^*_{C7=C8}$	25.6	25.2	19.5	19.3	20.9	20.8	18.8	18.7	20.1	20.0
$\pi_{C5=C6} \rightarrow \pi^*_{C2=O1}$	33.5	30.7	27.9	25.9	26.9	25.2	28.1	26.0	26.9	25.2
$LP_{O1(p)} \rightarrow \sigma^*_{C2-C3}$	25.5	28.4	26.0	28.5	25.6	28.1	26.0	28.5	25.5	28.0
$LP_{O1(p)} \rightarrow \sigma^*_{C2-C5}$	23.1	23.7	23.5	24.3	24.6	25.4	23.5	24.4	24.9	25.7
$LP_{Z4(p)} \rightarrow \pi^*_{C2=O1}$	2.0	----[a]	2.1	----	2.3	----	2.1	----	2.3	----
$LP_{Z4(p)} \rightarrow \sigma^*_{C2-C3}$	5.0	6.9	3.9	5.8	3.8	5.8	4.0	5.8	3.7	5.8
$LP_{Z4(p)} \rightarrow \sigma^*_{C2-C5}$	---	0.7	----	0.6	----	0.6	----	0.6	----	0.6
$\sigma_{C3-Z4} \rightarrow \pi^*_{C2=O1}$	4.6	----	6.7	----	7.2	----	6.6	----	7.2	----
$\pi_{C2-O1} \rightarrow \sigma^*_{C3-Z4}$	3.1	----	3.4	----	3.4	----	3.4	----	3.4	----
$LP_{O1(p)} \rightarrow \sigma^*_{C8-X9}$	0.6	0.6	0.7	0.8	----	----	0.8	0.8	----	----
$LP_{O1(p)} \rightarrow \sigma^*_{C5-X9}$	----	----	----	----	1.3	1.3	----	----	1.3	1.4
$\sigma_{C3-Z4} \rightarrow \sigma^*_{C2-C5}$	----	2.7	----	3.4	----	----	----	3.5	----	----
$LP_{O1(p)} \rightarrow \sigma^*_{C15-H16}$	0.8	0.9	----	----	----	----	----	----	----	----
$\sum$	265.6	261.1	210.4	205.6	209.5	198.9	207.1	202.6	206.1	195.6

[a] Interaction energy lower than 0.5 kcal mol^{-1}.

Table 8b

Selected NBO interaction energies (kcal. mol^{-1}) for compounds **2-5** calculated at M05-2X/aug-cc-pVTZ level.

Orbitals	X=O, Y=H, Z=Cl (**2**)				X=O, Y=H, Z=Br(**3**)				X=O, Y=Me, Z=Br(**4**)				X=O, Y=NO_2, Z=Br (**5**)			
	ac(syn)	*sp(syn)*	*ac(anti)*	*sp(anti)*	*ac(syn)*	*sp(syn)*	*ac(anti)*	*sp(anti)*	*ac(syn)*	*sp(syn)*	*ac(anti)*	*sp(anti)*	*ac(syn)*	*sp(syn)*	*ac(anti)*	*sp(anti)*
$LP_{X9(p)} \rightarrow \pi^*_{C7=C8}$	40.9	40.5	39.1	38.1	40.9	40.5	38.9	34.9	43.7	43.3	41.7	40.6	42.7	42.5	40.7	40.1
$LP_{X9(p)} \rightarrow \pi^*_{C5=C6}$	37.1	38.1	35.3	34.9	37.3	38.0	35.2	38.2	35.7	36.4	33.6	33.1	38.2	38.9	36.5	36.2
$\pi_{C7=C8} \rightarrow \pi^*_{C5=C6}$	20.2	24.8	24.9	24.5	20.2	24.9	24.9	24.6	27.0	26.6	18.5	23.4	22.3	22.1	24.2	21.8
$\pi_{C5=C6} \rightarrow \pi^*_{C7=C8}$	25.3	20.0	21.2	21.1	25.2	20.0	21.3	21.1	17.6	17.4	27.6	18.5	22.9	22.6	21.8	24.2
$\pi_{C5=C6} \rightarrow \pi^*_{C2=O1}$	26.2	24.3	25.9	24.4	26.1	24.3	25.9	24.5	27.8	25.7	25.4	25.9	21.7	20.3	21.2	20.3
$LP_{O1(p)} \rightarrow \sigma^*_{C2-C3}$	26.0	28.9	26.1	28.5	25.7	28.2	25.5	27.8	25.7	28.2	25.3	27.9	25.6	27.9	25.1	27.1
$LP_{O1(p)} \rightarrow \sigma^*_{C2-C5}$	26.5	27.3	25.5	25.9	26.8	27.6	25.6	26.1	26.2	27.1	25.3	25.8	28.4	29.9	27.0	27.3
$LP_{Z4(p)} \rightarrow \pi^*_{C2=O1}$	1.7	----[a]	2.4	----	2.0	----	2.5	----	1.9	----	3.7	----	2.1	----	2.9	----
$LP_{Z4(p)} \rightarrow \sigma^*_{C2-C3}$	5.2	7.0	4.8	6.9	4.0	5.8	3.7	5.7	4.0	5.7	----	5.7	4.1	5.9	3.7	5.8
$LP_{Z4(p)} \rightarrow \sigma^*_{C2-C5}$	-----	0.7	----	0.7	----	0.6	----	0.7	----	0.6	7.2	0.7	----	0.7	----	0.7
$\sigma_{C3-Z4} \rightarrow \pi^*_{C2=O1}$	4.0	----	5.1	----	6.4	----	7.5	----	3.4	----	6.2	----	6.4	----	8.2	----
$\pi_{C2-O1} \rightarrow \sigma^*_{C3-Z4}$	3.2	----	3.1	----	3.5	----	3.3	----	3.5	----	3.4	----	3.4	----	3.2	----
$LP_{O1(p)} \rightarrow \sigma^*_{C8-X9}$	0.5	0.5	----	----	0.5	0.5	----	----	0.5	0.5	----	----	0.6	0.6	----	----
$LP_{O1(p)} \rightarrow \sigma^*_{C5-X9}$	----	----	1.4	1.6	----	----	1.5	1.6	----	----	----	----	-----	----	1.7	1.8
$\sigma_{C3-Z4} \rightarrow \sigma^*_{C2-C5}$	----	2.6	----	----	----	3.2	----	----	----	3.2	----	3.3	----	3.4	----	----
$LP_{O1(p)} \rightarrow \sigma^*_{C15-H16}$	----	----	----	----	----	----	----	----	----	----	----	----	----	----	----	----
$\sum$	216.8	214.7	214.8	206.6	218.6	213.6	215.8	205.2	217.0	214.7	217.9	204.9	218.4	214.8	216.2	205.3

[a] Interaction energy lower than 0.5 kcal mol^{-1}.

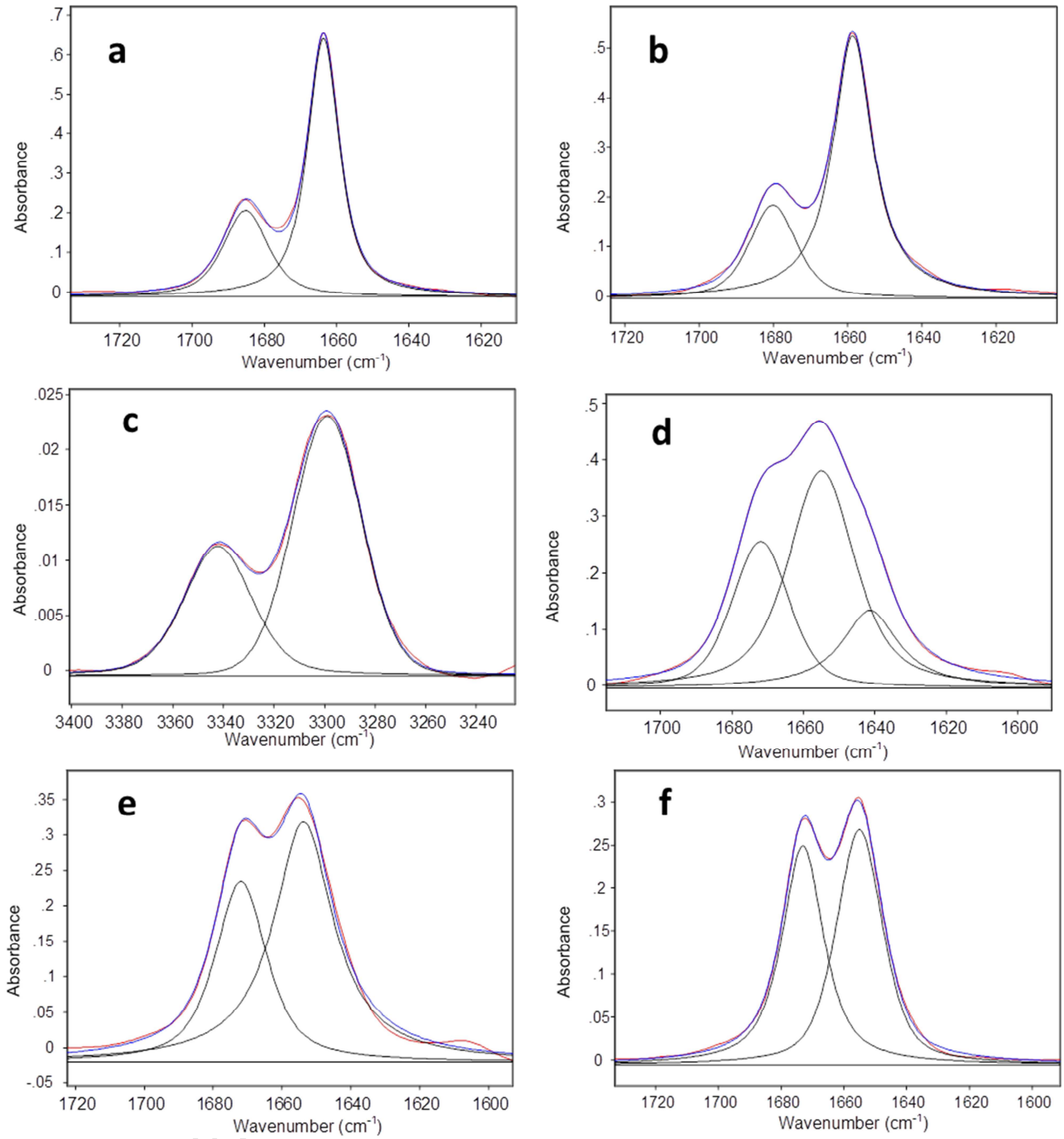

Fig.1. IR spectra of 2-(-2'-chloroacetyl)-1-methylpyrrole (**1**) showing the carbonyl stretching band in *n*-hexane (a), carbon tetrachloride [fundamental (b) and first overtone (c)], chloroform (d), dichloromethane (e) and acetonitrile (f). The red line is the experimental band; the blue line is the fitted band; the black lines are the band components.

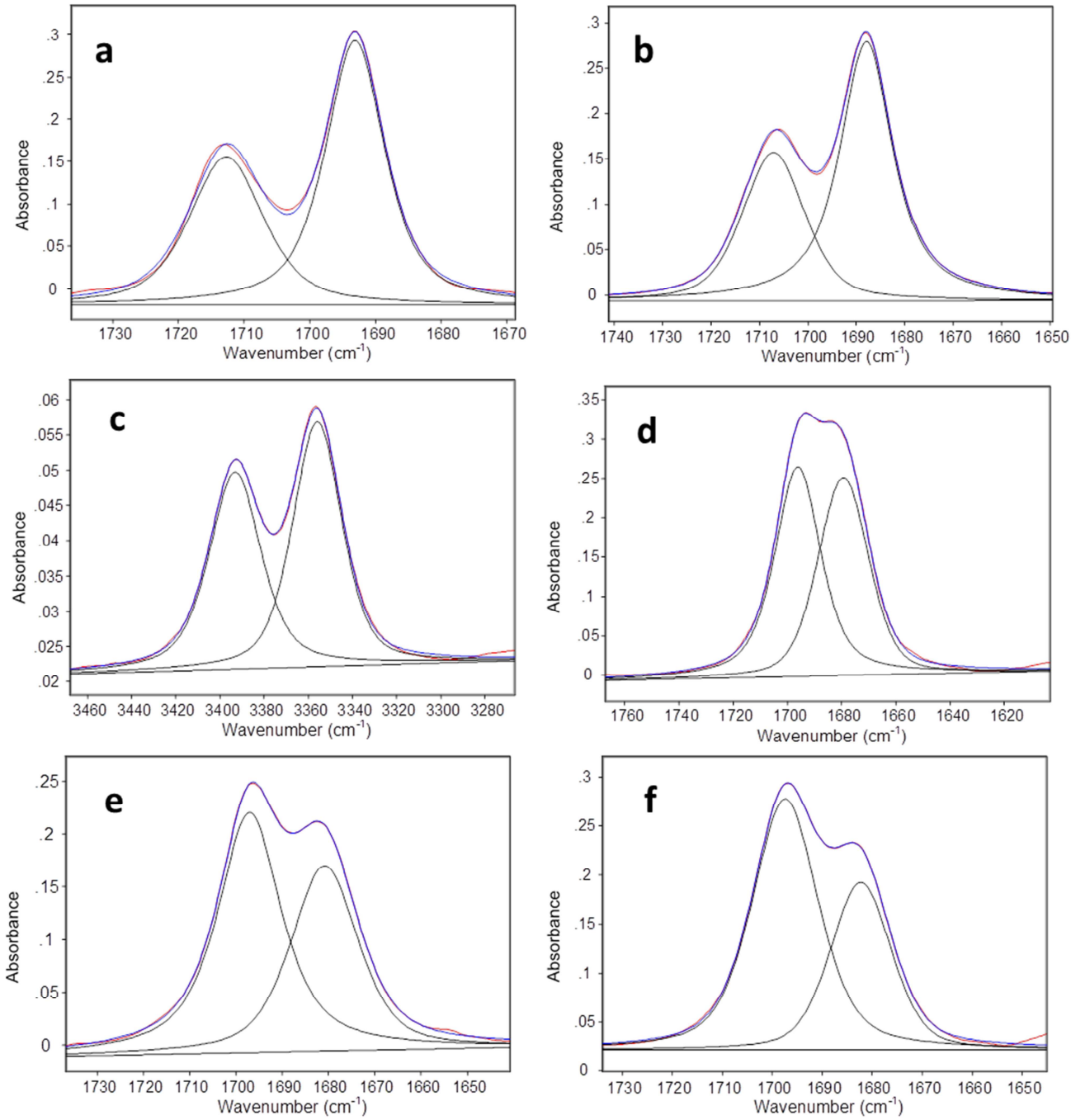

Fig. 2. IR spectra of 2-(2'-chloroacetyl)furan(**2**) showing the carbonyl stretching band in *n*-hexane (a), carbon tetrachloride [fundamental (b) and first overtone (c)], chloroform (d), dichloromethane (e) and acetonitrile (f). The red line is the experimental band; the blue line is the fitted band; the black lines are the band components.

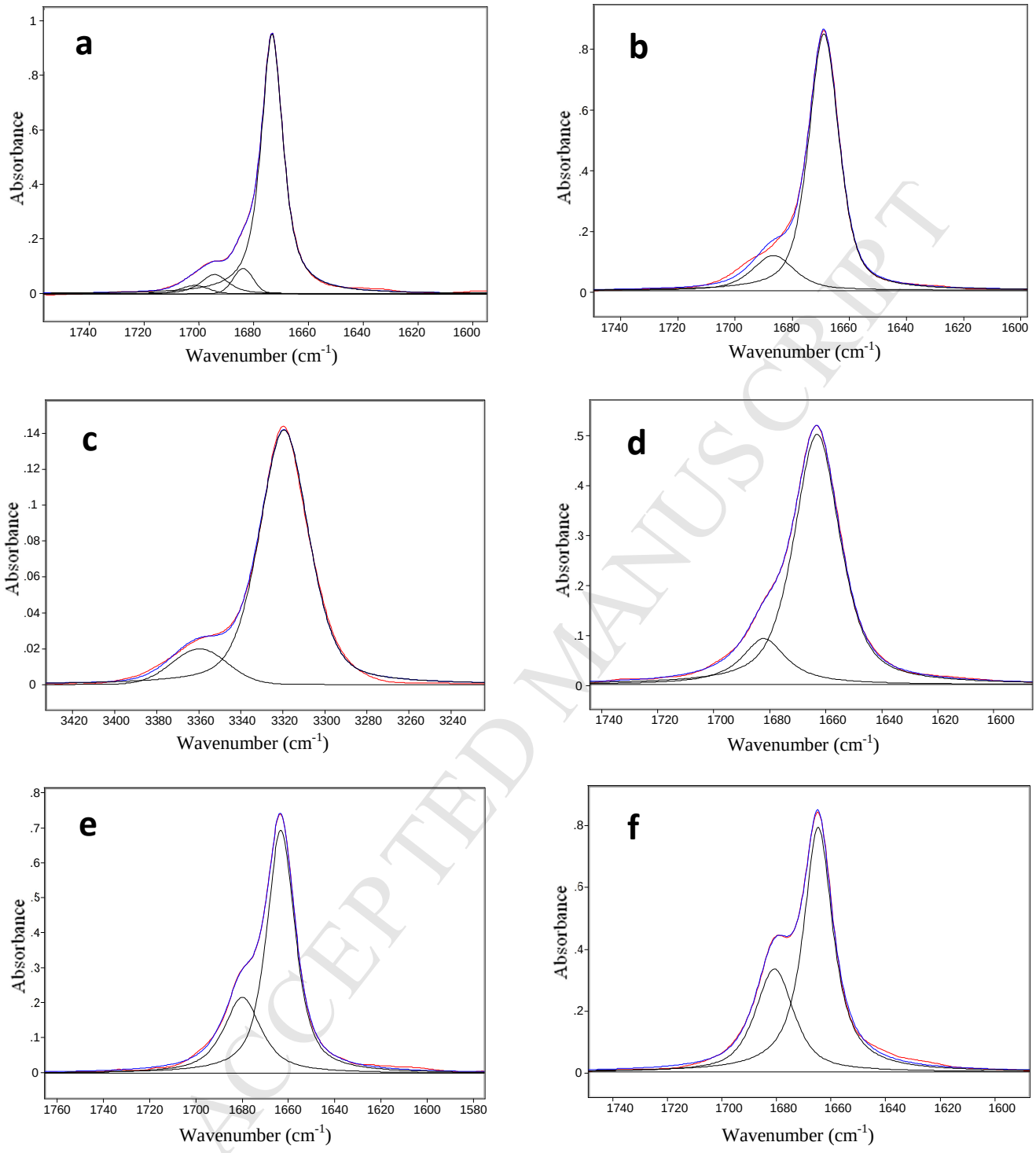

Fig.3. IR spectra of 2'(-2-bromoacetyl)-5-chlorothiophene (**7**) showing the carbonyl stretching band in *n*-hexane (a), carbon tetrachloride [fundamental (b) and first overtone (c)], chloroform (d), dichloromethane (e) and acetonitrile (f). The red line is the experimental band; the blue line is the fitted band; the black lines are the band components.

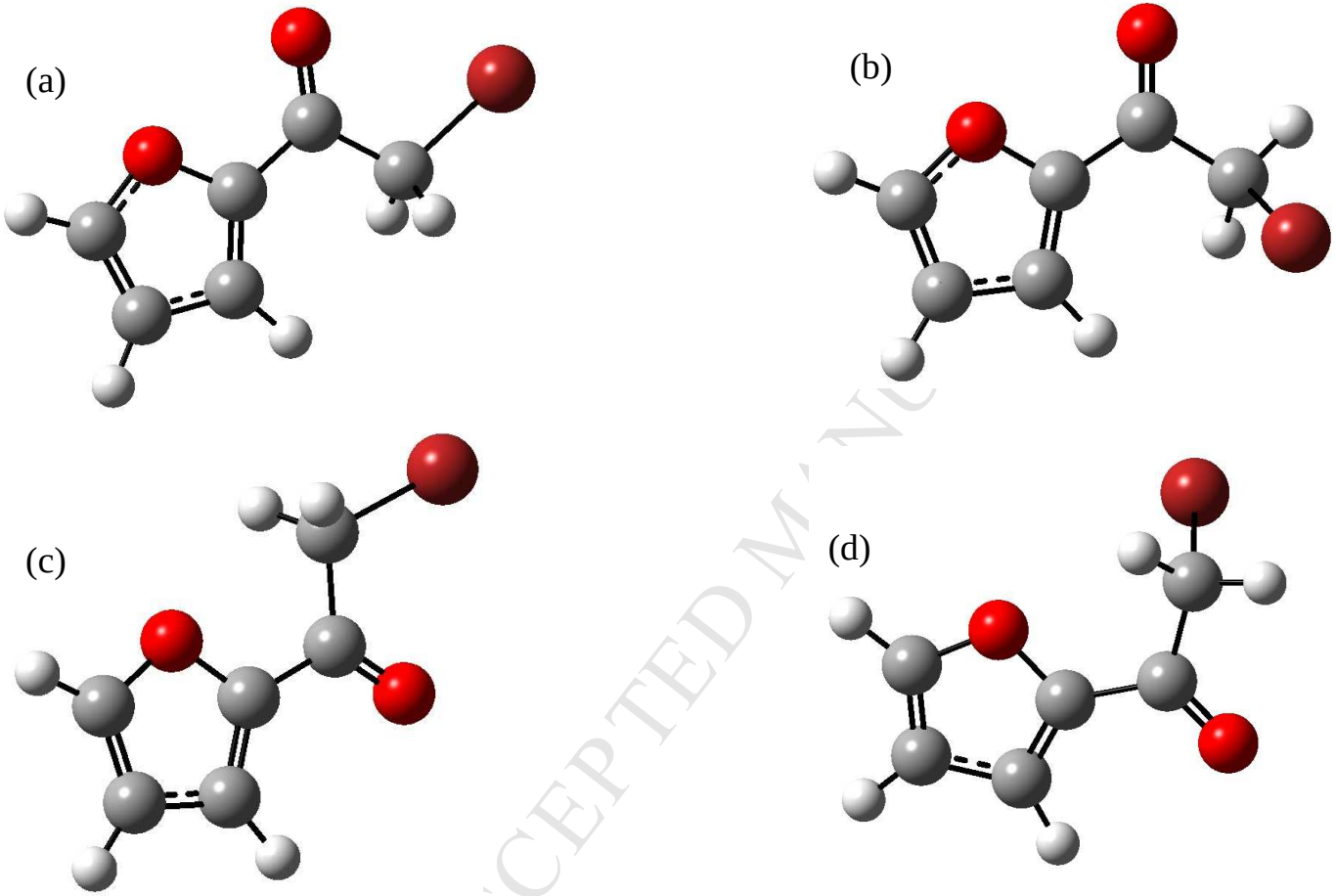

Fig. 4. *sp*(*syn*) (a), *ac*(*syn*) (b), *sp*(*anti*) (c) and *ac*(*anti*) (d) conformers of 2-(2'-bromoacetyl)furan (**3**) optimised at the M05-2x/aug-cc-pVTZ level.

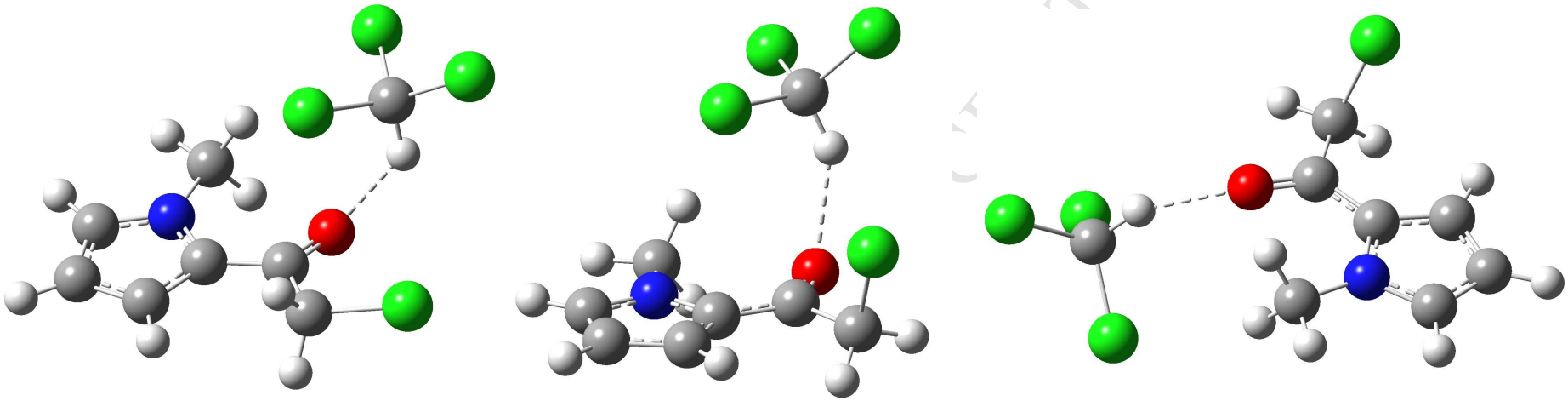

Complex 1 *Complex 2* *Complex 3*

Fig. 5. Structures of the hydrogen bonding complexes between 2-(2'-chloroacetyl)-pyrrole and chloroform obtained at the M05-2x/aug-cc-pVDZ level: *Complex 1* [*sp*(*syn*)…$HCCl_3$]; *Complex 2* [*ac*(*syn*)…$HCCl_3$]; *Complex 3* [*ac*(*syn*)…$HCCl_3$].

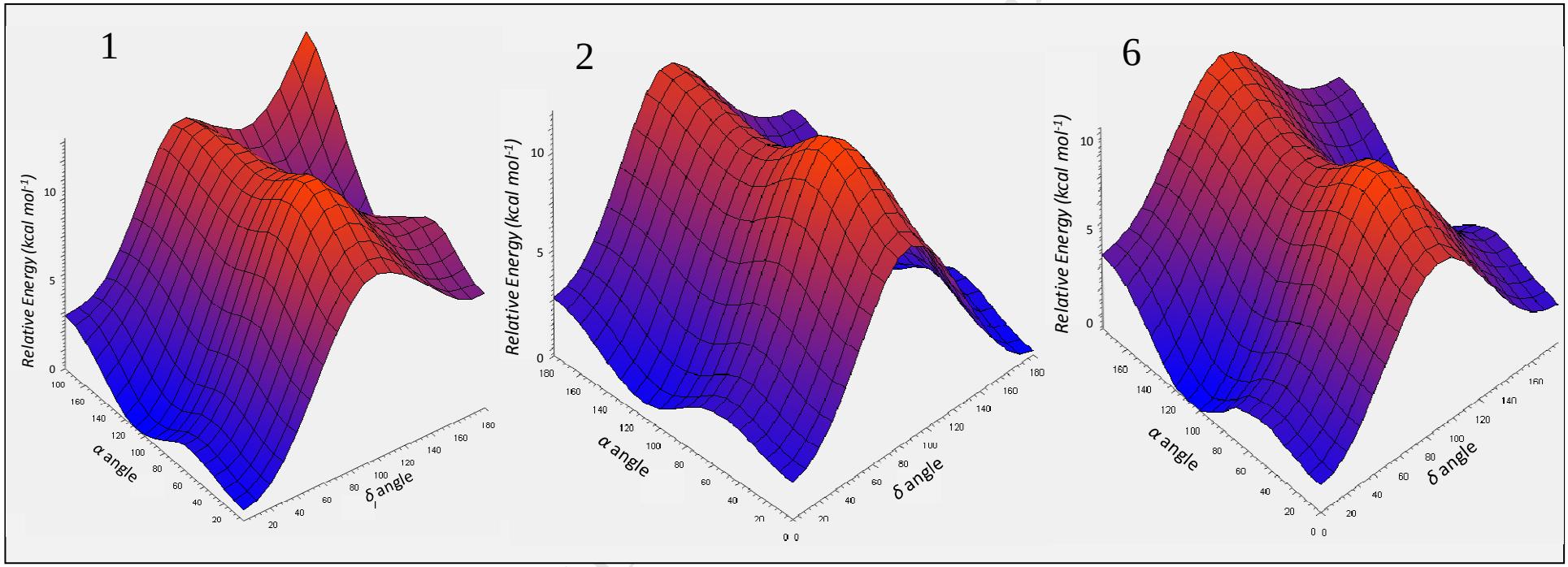

Fig. 6. Potential energy surfaces of compounds **1**, **2** and **6** obtained at the M05-2x/aug-cc-pVDZ level.

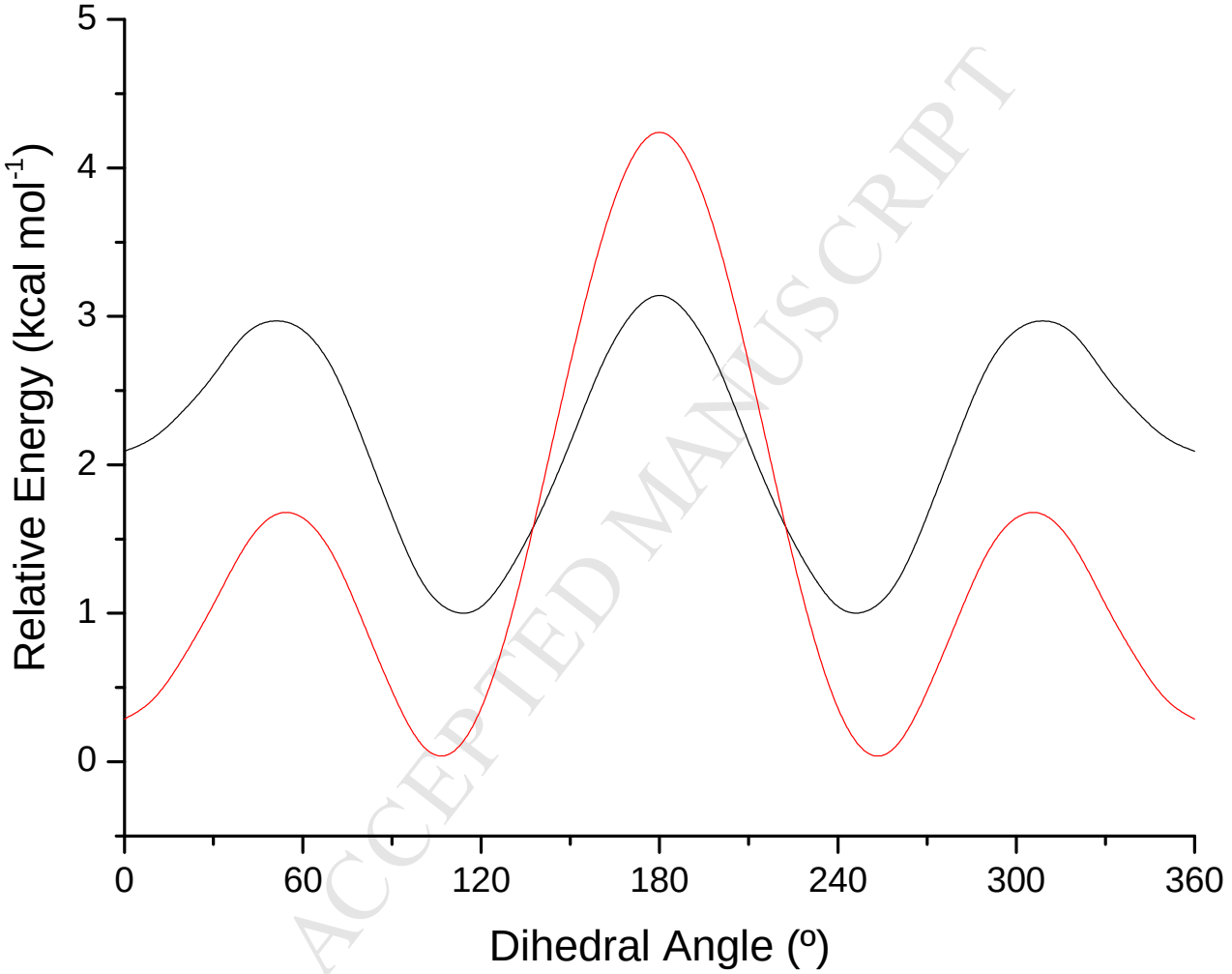

Fig. 7. One dimension potential energy surfaces of the α dihedral angle for compound **2** when δ dihedral angle is 0º (black line) or 180º (red line).

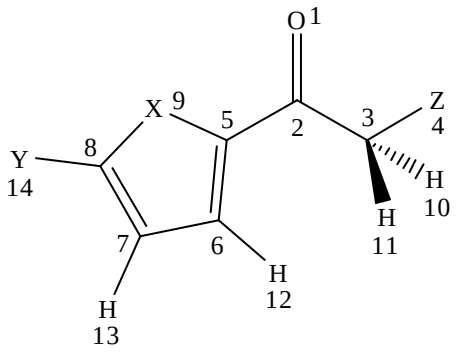

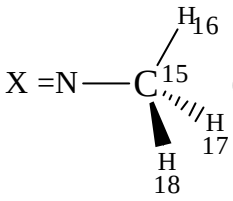

(**1**), O (**2**-**5**), S (**6**,**7**)

Y = H (**1**-**3**,**6**), Me (**4**) NO_2 (**5**), Cℓ (**7**)

Z = Cℓ (**1**,**2**), Br (**3**-**7**)

α = O(1)=C(2)-C(3)-Z(4)

δ = O(1)=C(2)-C(5)-X(9)

Scheme 1. Atom labelling of 2-(2'-haloacetyl)-5-substituted five-membered heteroaromatic compounds Z–$CH_2C(O)(C_4H_2X)$–Y (**1**–**7**) and definition of the relevant dihedral angles.

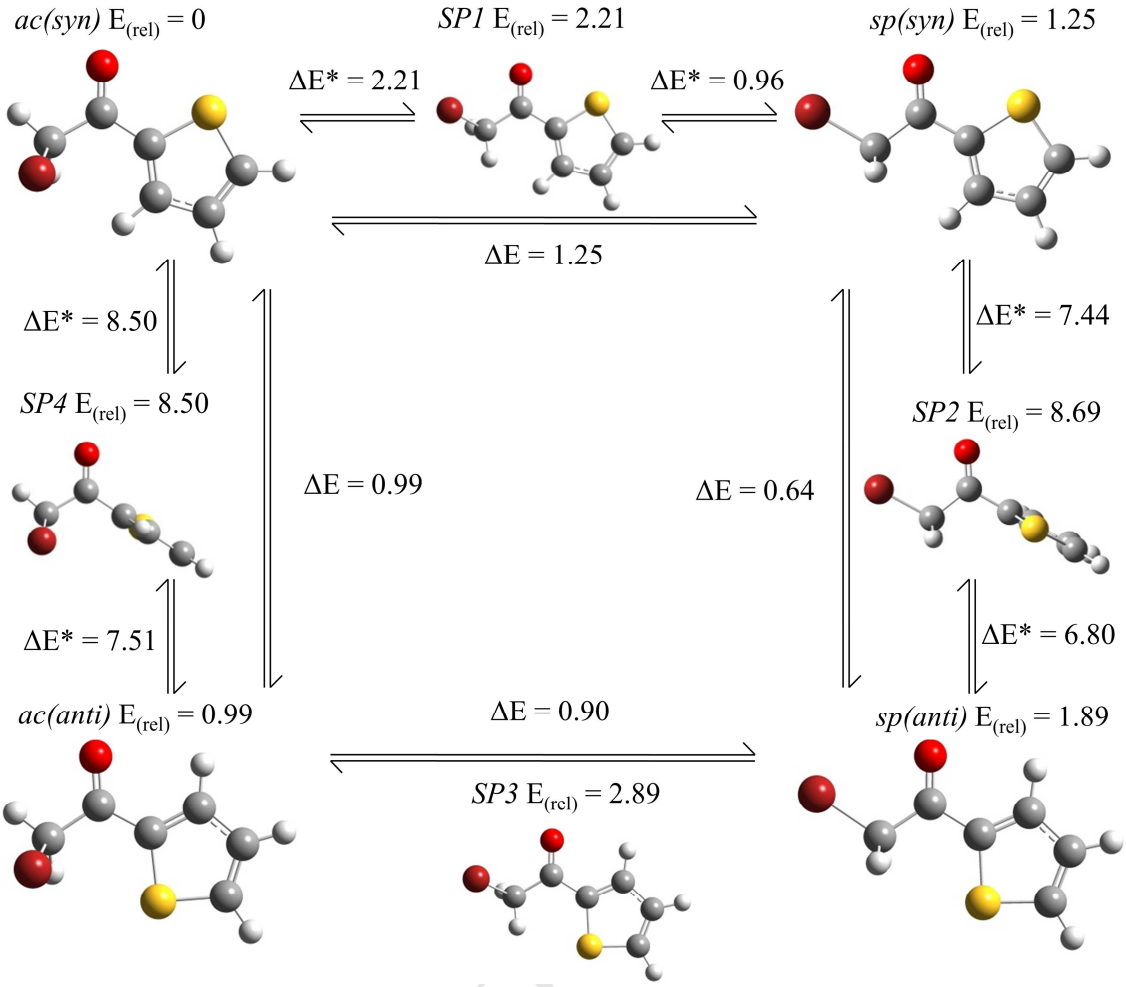

Scheme 2. Inter-conversion of the four conformers of 2-(-2'-bromoacetyl)thiophene. All energy values are in kcal mol^{-1}. $E_{(Rel)}$ indicates the energy relative to the minimum energy structure *ac*(*syn*). ΔE refers to the proper energy difference between two conformers. ΔE* refers to the energy difference between a minimum structure and that of a saddle point.

Highlights

- Calculations predict for **1**-**7**: *ac*(*syn*), *sp*(*syn*), *ac*(*anti*) and *sp*(*anti*) conformers.
- IR of **1**-**6** in solution indicate two pairs of conformers: *ac*(*syn*)/*sp*(*syn*); *ac*(*anti*)/*sp*(*anti).*
- In *n*-hexane the 2'-bromoacetyl-thiophene **7** displays four conformers.
- C=O…$HCCl_3$ complexes justifyIR triplets found in chloroform for **1**,**3**,**5**.
- A good match was found between the experimental and theoretical data.
- Conformer stability and frequency are controlled by coulombic and orbital interaction.